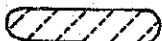
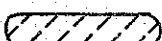


LEGEND

Presumed Soil Classification
about 100m width of riverside along the river

- GP, SP, ML etc. : Soil Symbol of Unified Soil Classification
- ← GP/SP → : Range of Soil Classification
- GP/SP : GP with SP
- SP(/ML) : Mostly SP with Minor ML

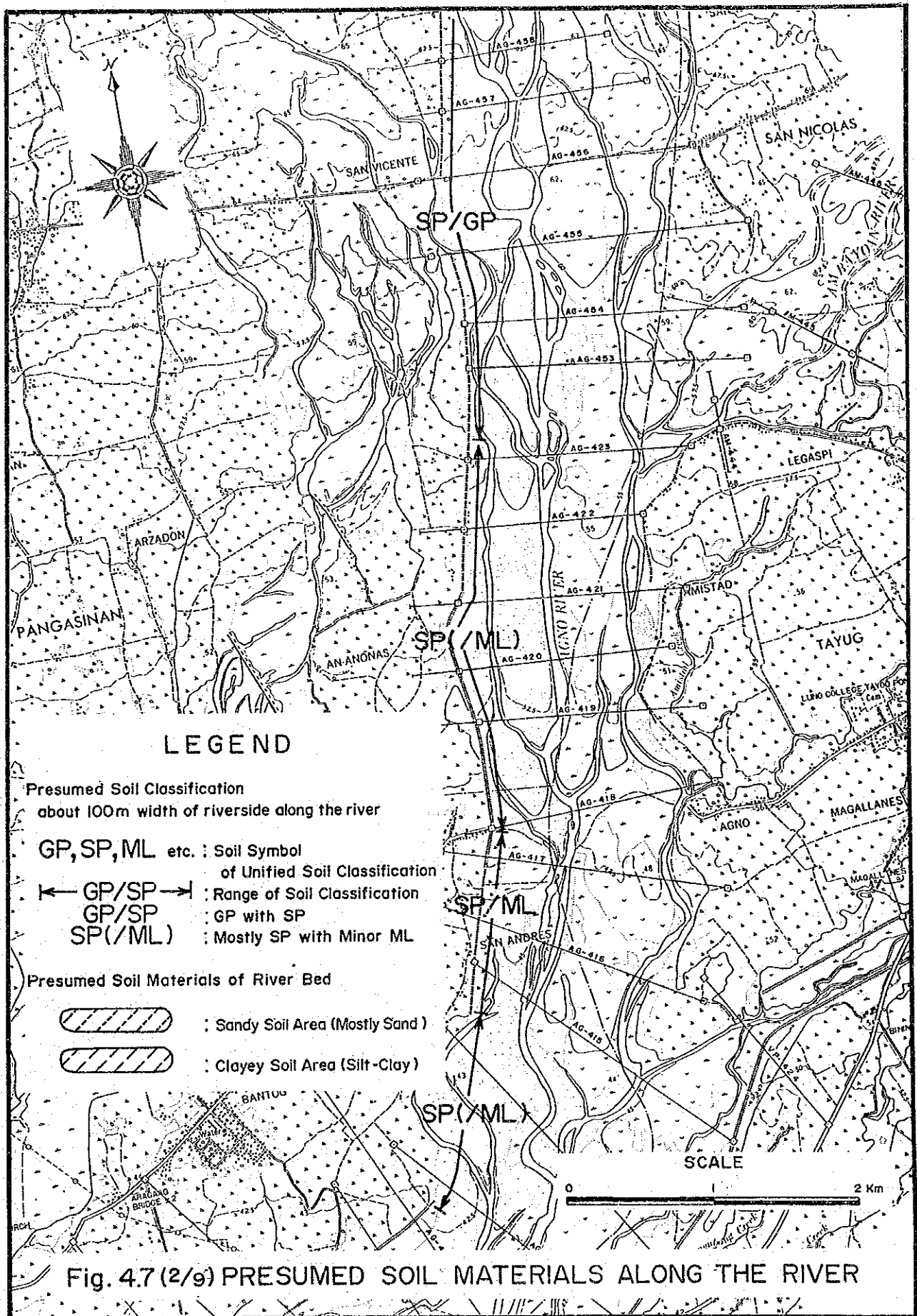
Presumed Soil Materials of River Bed

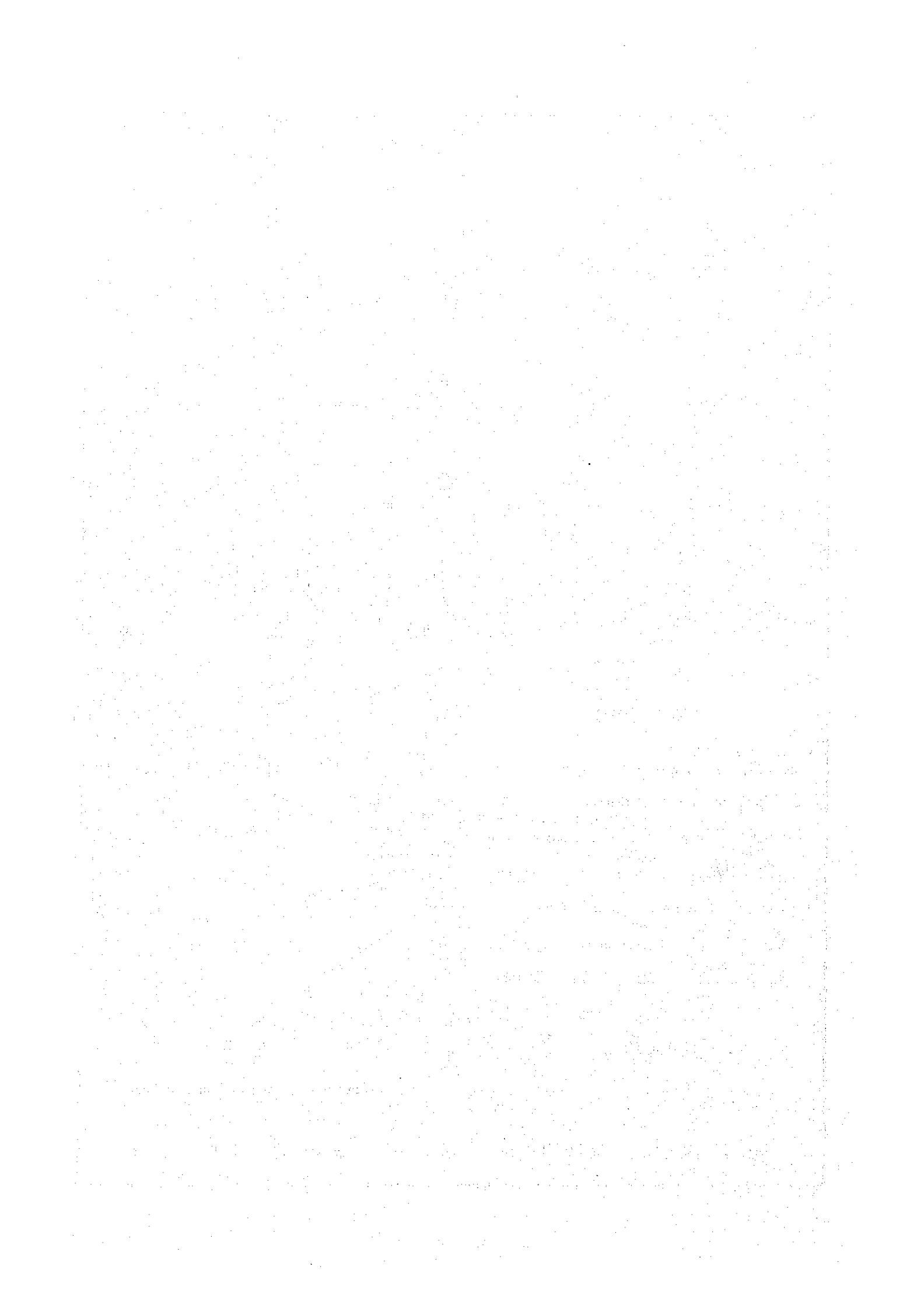
-  : Sandy Soil Area (Mostly Sand)
-  : Clayey Soil Area (Silt-Clay)

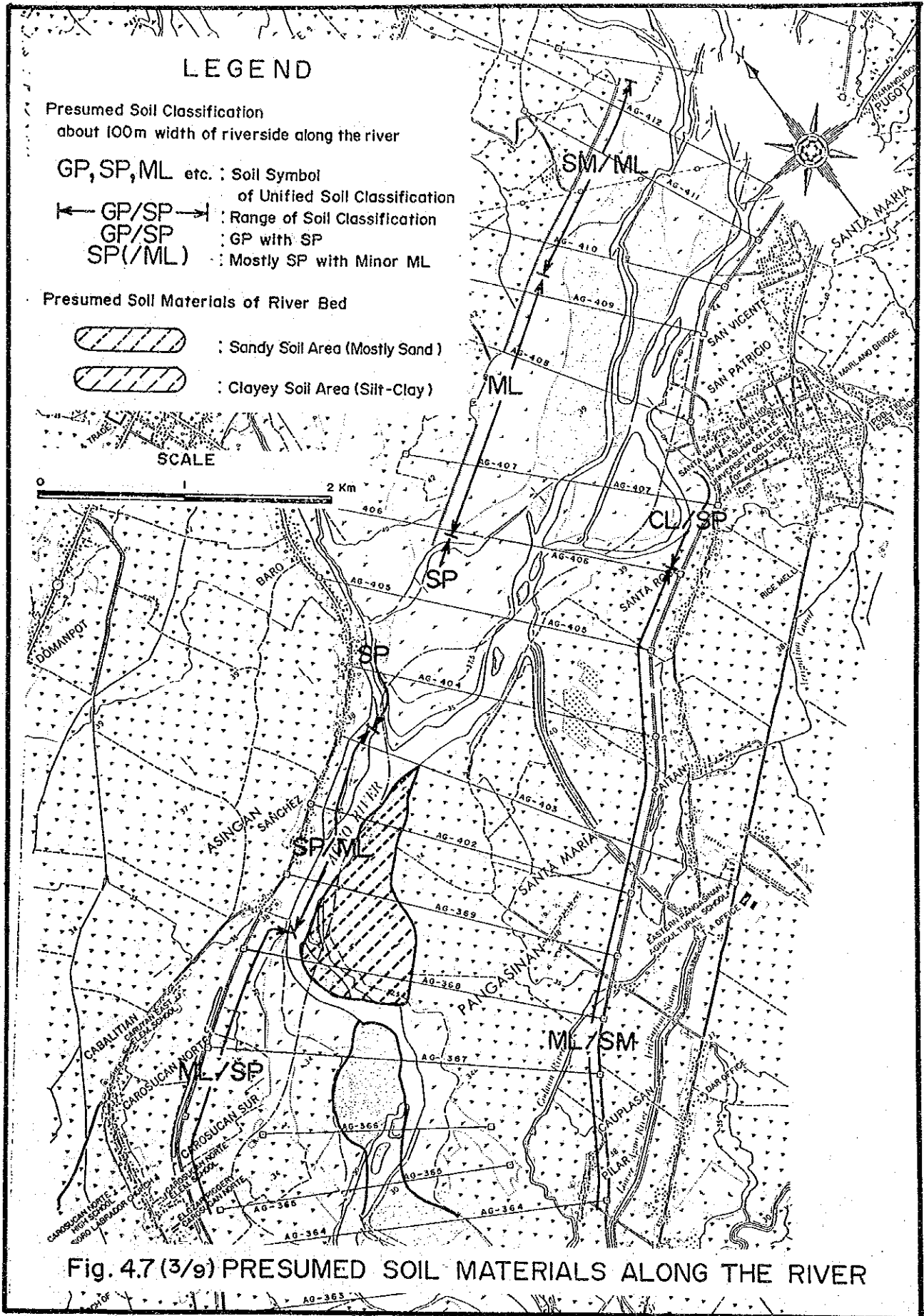
SCALE

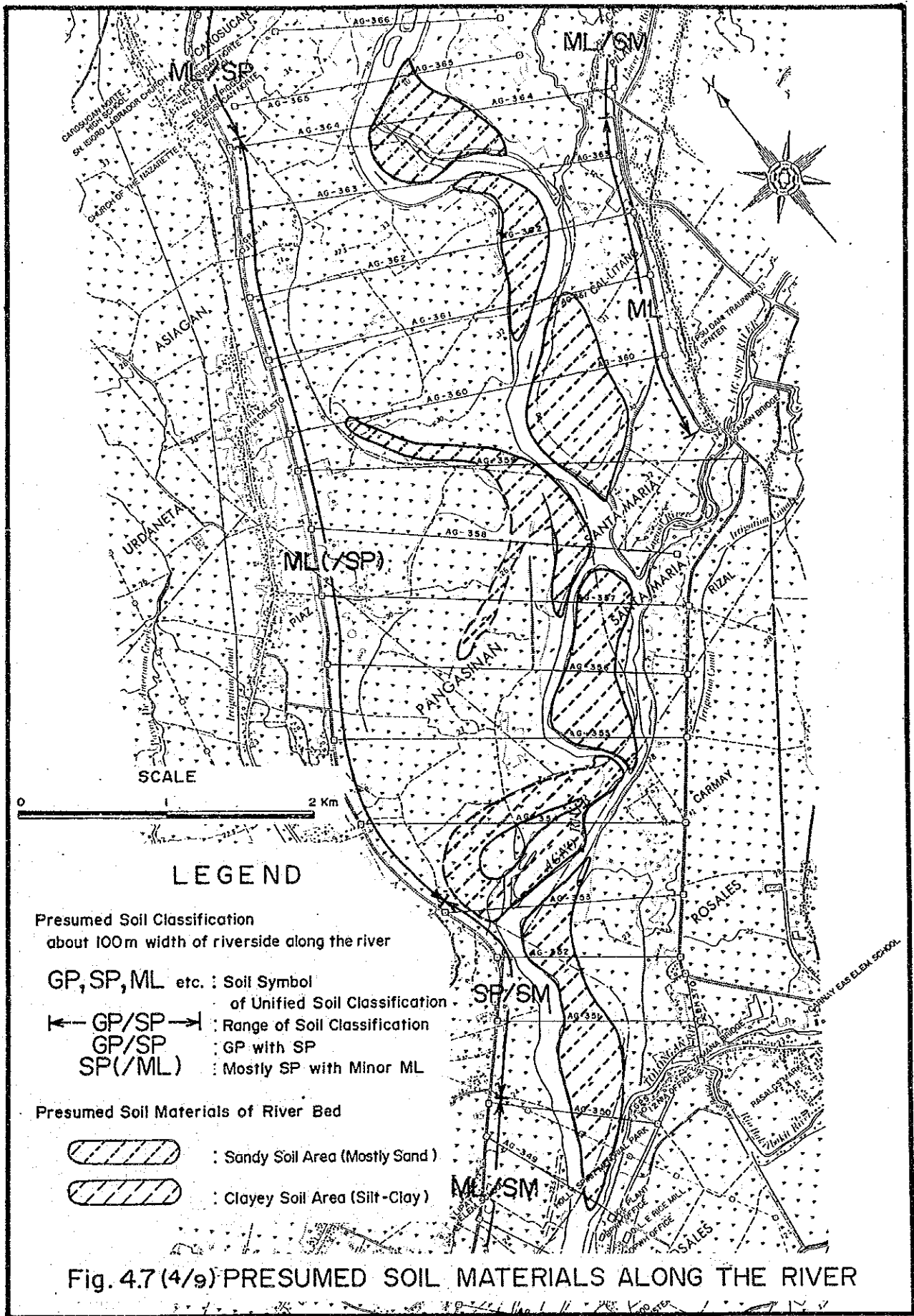
0 2 Km

Fig. 4.7 (1/9) PRESUMED SOIL MATERIALS ALONG THE RIVER









LEGEND

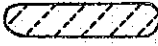

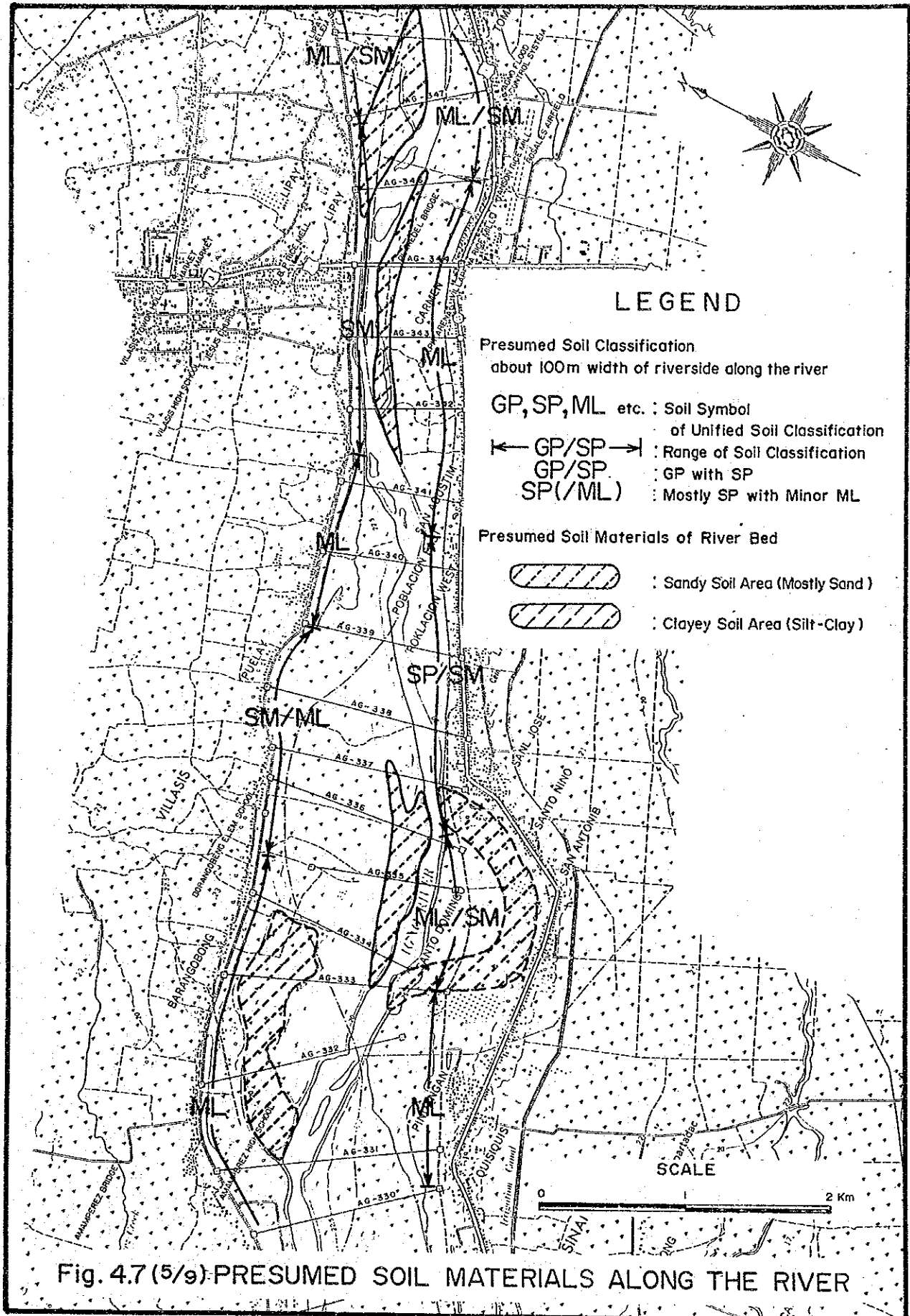
- Presumed Soil Classification
about 100m width of riverside along the river
- GP, SP, ML etc. : Soil Symbol
of Unified Soil Classification
- ← GP/SP → : Range of Soil Classification
GP/SP : GP with SP
SP(/ML) : Mostly SP with Minor ML
- Presumed Soil Materials of River Bed
-  : Sandy Soil Area (Mostly Sand)
 : Clayey Soil Area (Silt-Clay)

Fig. 4.7(4/9) PRESUMED SOIL MATERIALS ALONG THE RIVER



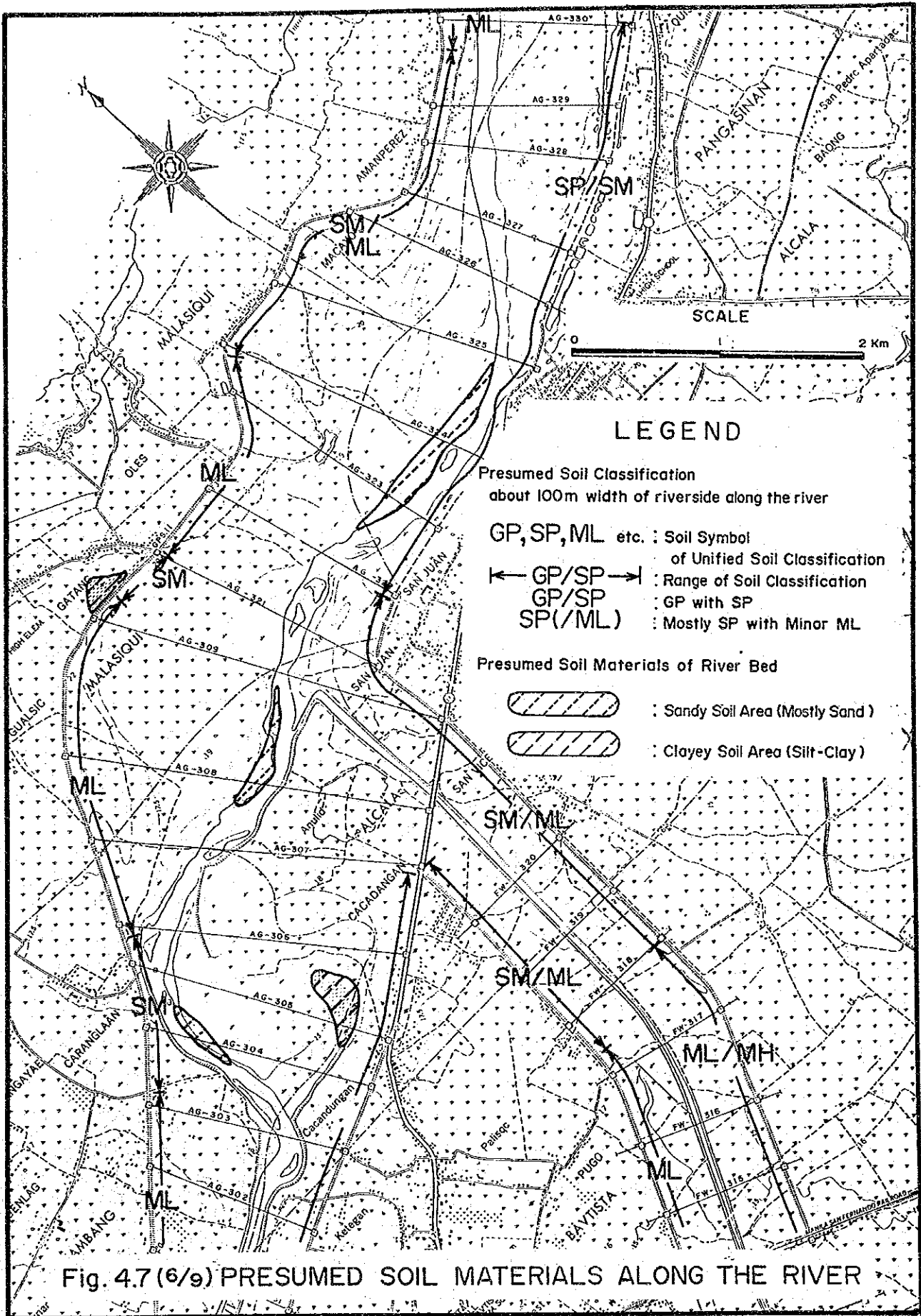
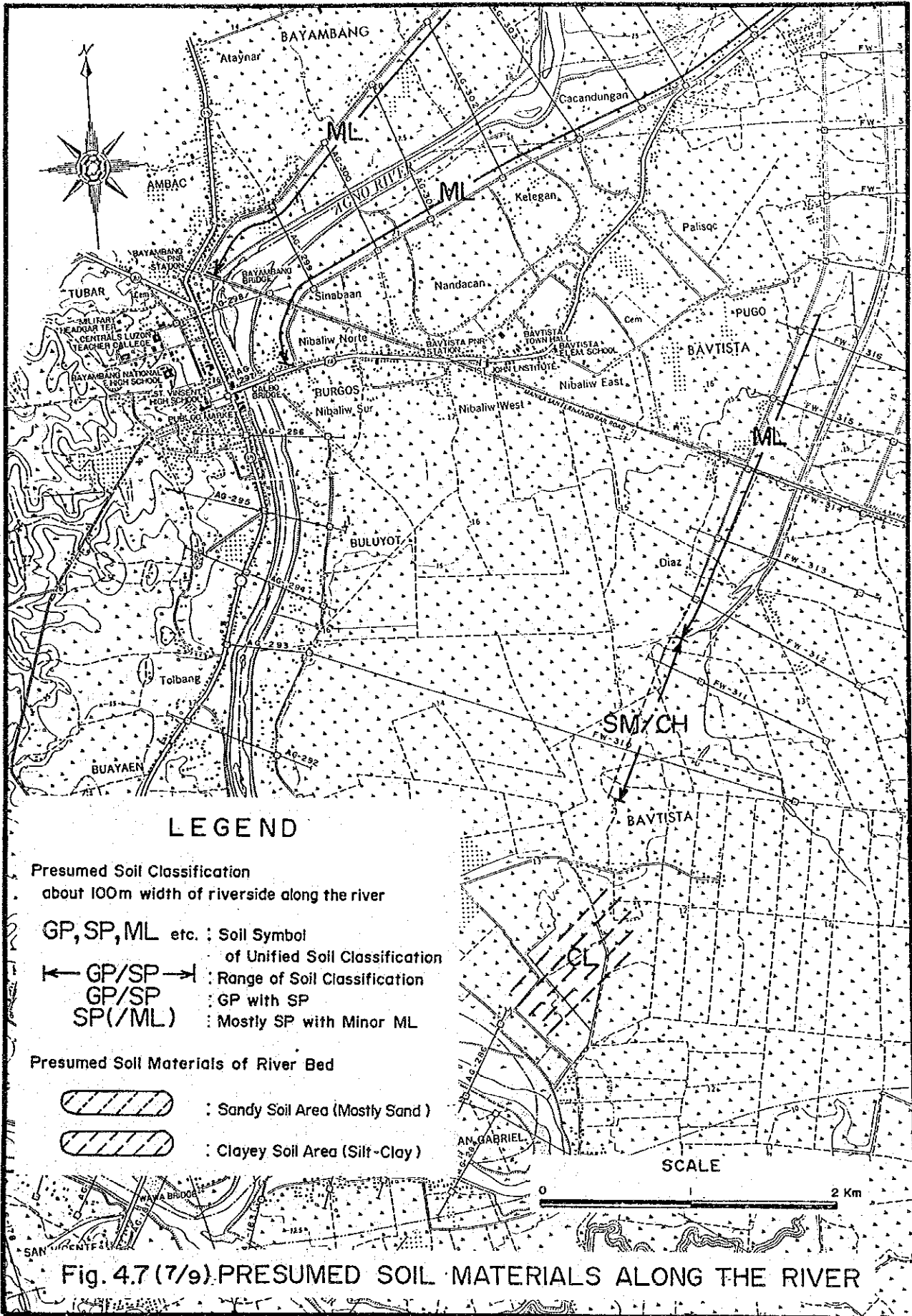
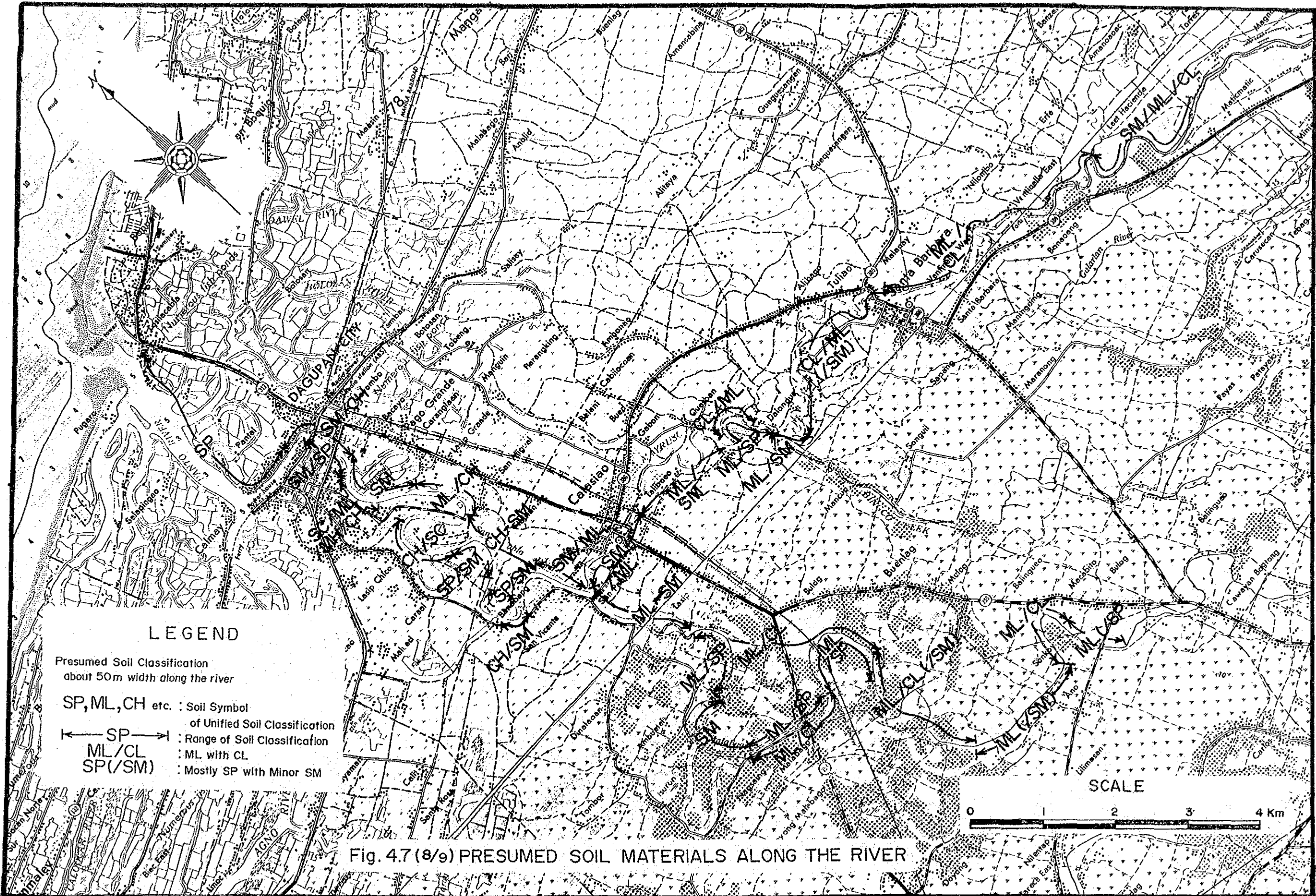


Fig. 4.7 (6/9) PRESUMED SOIL MATERIALS ALONG THE RIVER





LEGEND

Presumed Soil Classification
about 50m width along the river

SP, ML, CH etc. : Soil Symbol
of Unified Soil Classification

← SP → : Range of Soil Classification

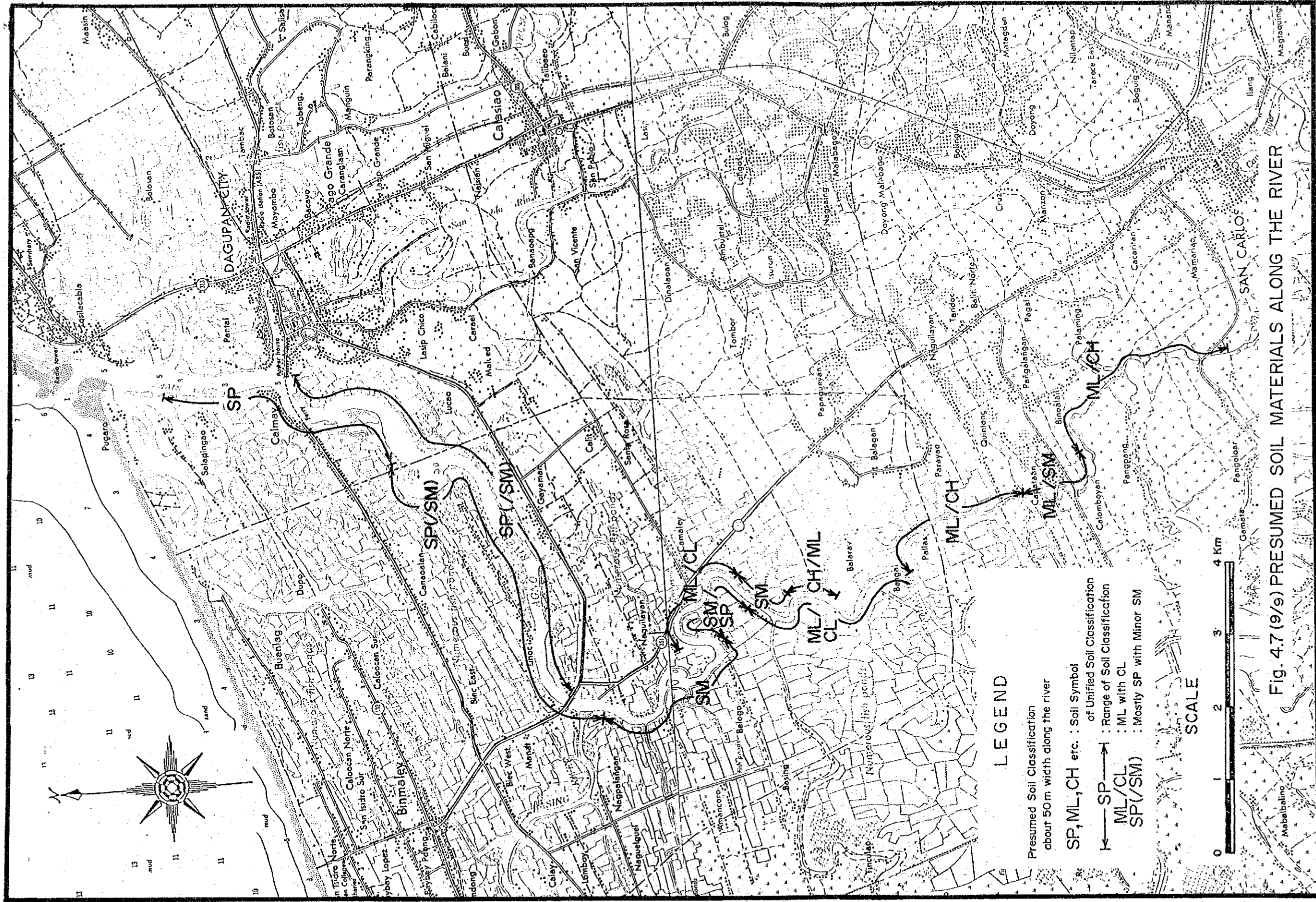
ML/CL : ML with CL

SP(/SM) : Mostly SP with Minor SM

Fig. 4.7 (8/9) PRESUMED SOIL MATERIALS ALONG THE RIVER

SCALE





LEGEND

Presumed Soil Classification about 50m width along the river

- SP, ML, CH etc. : Soil Symbol of Unified Soil Classification
- ML/CL : Range of Soil Classification
- SP/SM : ML with CL
- ML/CH/ML : Mostly SP with Minor SM

SCALE

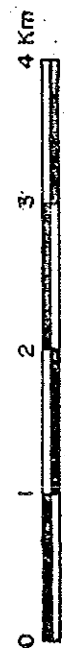


Fig. 4.7 (9/9) PRESUMED SOIL MATERIALS ALONG THE RIVER

4. LF
LIQUEFACTION
STUDY

LF: LIQUEFACTION STUDY

TABLE OF CONTENTS

	<u>Page</u>
1. SUMMARY	LF.1
2. OBJECTIVE	LF.3
3. LIQUEFACTION PHENOMENA	LF.4
3.1 General	LF.4
3.2 Earthquake Motion Causes Liquefaction	LF.4
3.3 Liquefaction Mechanism Induced by Cyclic Shear	LF.5
4. EARTHQUAKE	LF.7
4.1 16 July 1990 Earthquake	LF.7
4.2 Recorded Earthquakes in the Study Area	LF.7
4.3 Fault	LF.8
5. STUDY ON CASE HISTORY	LF.9
5.1 Earthquake Damage of River Dikes	LF.9
5.2 Damage of River Structures by 1978 Miyagikenoki Earthquake	LF.10
5.3 Settlement of Earth Structures Caused by The Nihonkai-Chubu Earthquake	LF.13
5.4 Countermeasures against Liquefaction of Ground under River Dikes	LF.15
6. SITE RECONNAISSANCE	LF.20
6.1 Dagupan City Area	LF.20
6.2 Middle Agno River	LF.23

7.	FIELD INVESTIGATION AND LABORATORY TEST	LF.27
7.1	Method	LF.27
7.2	Site Geology	LF.27
7.3	Laboratory Test Results	LF.29
8.	ANALYSIS OF LIQUEFACTION	LF.32
8.1	Methodology	LF.32
8.2	Calculation of Liquefaction	LF.35
8.3	Evaluation on Liquefaction	LF.36
9	COUNTERMEASURES AGAINST LIQUEFACTION FOR RIVER STRUCTURES	LF.37
9.1	Basic Concept	LF.37
9.2	Selection of Countermeasures	LF.38
9.3	Recommended Countermeasures	LF.40
10.	CONCLUSION AND RECOMMENDATION	LF.41
10.1	Conclusion	LF.41
10.2	Recommendation	LF.44
11.	REFERENCES	LF.45

LIST OF TABLES

<u>No</u>		<u>Page</u>
5.1	DAMAGED SHAPE OF RIVER DIKE	LF.47
5.2	DAMAGED PLACES AND LENGTH IN EACH RIVER	LF.47
5.3	FEATURE OF DAMAGE DIKE	LF.48
5.4	DAMAGE QUANTITY OF RIVER DIKE	LF.48
5.5	DAMAGED DIKE BY CLASSIFICATION OF MICRO - TOPOGRAPHY	LF.49
5.6	OCCURRENCE RATE OF SAND BOIL AT DAMAGED LOCATION OF RIVER DIKE	LF.50
5.7	COMPARISON OF COMPACTION METHODS	LF.51
7.1	QUANTITY OF ADDITIONAL CORE BORING AND LABORATORY TEST	LF.52
7.2	PHYSICAL PROPERTIES OF GROUND IN DAGUPAN CITY AREA	LF.53
7.3	PHYSICAL PROPERTIES OF GROUND IN MIDDLE AGNO RIVER BASIN ...	LF.54
7.4	FEATURE OF SAND DEPOSIT	LF.55
7.5	COEFFICIENT OF UNIFORMITY AND CURVATURE	LF.56
8.1	ASSUMED VALUE OF DENSITY AND MEAN PARTICLE SIZE BY SOIL CLASSIFICATION	LF.57
8.2	LIQUEFIED DEPTH FROM GROUND SURFACE	LF.57
9.1	COMPARISON OF COUNTERMEASURE METHOD AGAINST LIQUEFACTION ...	LF.58
9.2	COMPARISON OF COST OF COUNTERMEASURE METHOD	LF.59

LIST OF FIGURES (1/3)

<u>No</u>		<u>Page</u>
3.1	EXPLANATION ON TRAVEL OF EARTHQUAKE WAVE	LF.60
3.2	ACTING FORCE TO SOIL ELEMENT BY P WAVE AND S WAVE	LF.61
3.3	LIQUEFACTION MECHANISM	LF.62
3.4	DAMAGE PATTERN INDUCED BY LIQUEFACTION	LF.63
4.1	DISTRIBUTION OF EARTHQUAKE GENERATORS IN THE PHILIPPINES ...	LF.64
4.2	ISOSEISMAL MAP OF THE 16 JULY 1990 EARTHQUAKE	LF.65
4.3	RELATION BETWEEN SEISMIC INTENSITY AND ACCELERATION	LF.66
5.1	SETTLEMENT OF DAMAGED RIVER DIKES	LF.67
5.2	DAMAGED SHAPES OF RIVER DIKES	LF.68
5.3	SETTLEMENT OF DAMAGED RIVER DIKES	LF.69
5.4	LOCATION OF EPICENTER AND INTENSITY	LF.70
5.5	SEVEN RIVERS IN MIYAGI-KEN	LF.71
5.6	LOCATION OF DAMAGED PLACE	LF.72
5.7	DAMAGE OF RIVER DIKE	LF.73
5.8	SAND BOIL POINT	LF.74
5.9	SAND BOIL IN OLD RIVER CHANNEL AT RIGHT BANK OF EAI RIVER ..	LF.75
5.10	DAMAGE LOCATION OF RIVER DIKE	LF.76
5.11	RELATION BETWEEN EPICENTER DISTANCE AND DAMAGE RATIO OF RIVER DIKE	LF.77
5.12	LOCATION MAP	LF.78
5.13	GEOLOGICAL CROSS SECTION	LF.79
5.14	RELATION BETWEEN MAXIMUM ACCELERATION AND UNIFORM CYCLIC STRESS RATIO CONVERTED BY 20 CYCLES	LF.80
5.15	UNLIQUEFIABLE RANGE OF N VALUE	LF.81
5.16	IMPROVEMENT RANGE	LF.82
5.17	RELATION BETWEEN N VALUE BEFORE AND AFTER IMPROVEMENT	LF.83
5.18	N VALUE BEFORE AND AFTER IMPROVED BY SAND COMPACTION PILE ..	LF.84
5.19	REHABILITATED SECTION OF EARTH DIKES	LF.85
5.20	LIQUEFACTION ANALYSIS ON HORIZONTAL GROUND	LF.86
5.21	LIQUEFACTION ANALYSIS IN TWO DIMENSIONAL SECTION (B SECTION)	LF.87
5.22	STUDIED COUNTERMEASURE RANGE (B SECTION)	LF.88
5.23	EFFECTIVENESS OF COUNTERMEASURE (B SECTION)	LF.89

LIST OF FIGURES (2/3)

<u>No</u>		<u>Page</u>
6.1	LOCATION MAP OF GEOLOGICAL SURVEY	LF.90
6.2	MAP SHOWING AFFECTED AND UNAFFECTED BUILDINGS BY LIQUEFACTION IN DAGUPAN CITY DURING THE 16 JULY NORTHERN LUZON EARTHQUAKES	LF.91
6.3	SKETCH OF DAMAGED MAGSAYSAY BRIDGE	LF.92
6.4	LOCATION OF DAMAGED SITE OF MAIN AGNO (1/2)	LF.93
6.5	LOCATION OF DAMAGED SITE OF MAIN AGNO (2/2)	LF.94
6.6	DAMAGED LEFT EARTHDIKE OF MAIN AGNO (Santa Maria - Tayug) .	LF.95
6.7	DAMAGED RIGHT EARTHDIKE OF MAIN AGNO (Bayambang - Carmen Bridge)	LF.96
6.8	SKETCH OF DAMAGED SISON BRIDGE	LF.97
6.9	SKETCH OF DAMAGED CALVO BRIDGE	LF.98
7.1	LOCATION MAP OF GEOLOGICAL SURVEY	LF.99
7.2	LOCATION MAP OF GEOLOGICAL SURVEY	LF.100
7.3	LOCATION MAP OF GEOLOGICAL SURVEY	LF.101
7.4	GEOTECHNICAL DATA OF DG - 1	LF.102
7.5	GEOTECHNICAL DATA OF DG - 3	LF.103
7.6	GEOTECHNICAL DATA OF DG - 5	LF.104
7.7	GEOTECHNICAL DATA OF MA - 2	LF.105
7.8	GEOTECHNICAL DATA OF MA - 5	LF.106
7.9	GEOTECHNICAL DATA OF MA - 6	LF.107
7.10	LEGEND	LF.108
7.11	GRADATION CURVE OF DG-1	LF.109
7.12	GRADATION CURVE OF DG-3	LF.110
7.13	GRADATION CURVE OF DG-5	LF.111
7.14	GRADATION CURVE OF MA-2	LF.112
7.15	GRADATION CURVE OF MA-5	LF.113
7.16	GRADATION CURVE OF MA-6	LF.114
7.17	COMPARISON BETWEEN SANDS IN STUDY AREA AND NIIGATA SAND	LF.115
7.18	GRADATION CURVE OF MIDDLE AGNO RIVER SAND (ASINGAN)	LF.116
8.1	FLOW OF LIQUEFACTION RESISTANT FACTOR FL OF DG-1	LF.117
8.2	EPICENTER AND FAULT OF 16 JULY 1990 EARTHQUAKE	LF.118
8.3	LIQUEFACTION RESISTANT FACTOR FL OF DG-1	LF.119
8.4	LIQUEFACTION RESISTANT FACTOR FL OF DG-3	LF.120
8.5	LIQUEFACTION RESISTANT FACTOR FL OF DG-5	LF.121

LIST OF FIGURES (3/3)

<u>No</u>		<u>Page</u>
8.6	LIQUEFACTION RESISTANT FACTOR FL OF MA-2	LF.122
8.7	LIQUEFACTION RESISTANT FACTOR FL OF MA-5	LF.123
8.8	LIQUEFACTION RESISTANT FACTOR FL OF MA-6	LF.124
8.9	LIQUEFIED LAYER OF DG-1	LF.125
8.10	LIQUEFIED LAYER OF DG-3	LF.126
8.11	LIQUEFIED LAYER OF DG-5	LF.127
8.12	LIQUEFIED LAYER OF DG-2	LF.128
8.13	LIQUEFIED LAYER OF DG-5	LF.129
8.14	LIQUEFIED LAYER OF DG-6	LF.130
9.1	SAND COMPACTION PILE METHOD (PROCESS)	LF.131
9.2	ROD COMPACTION METHOD	LF.132
9.3	DYNAMIC CONSOLIDATION METHOD	LF.133
9.4	DEEP MIXING METHOD (CONSTRUCTION SYSTEM)	LF.134
9.5	GRAVEL PILE METHOD	LF.135
9.6	DESIGN CHART OF SCP FOR SANDY SOIL	LF.136
9.7	SAND COMPACTION PILE METHOD	LF.137
9.8	TAMPING ENERGY AND INCREASED N VALUE BY DYNAMIC CONSOLIDATION	LF.138
9.9	DYNAMIC CONSOLIDATION METHOD	LF.139
9.10	DEEP MIXING METHOD	LF.140
9.11	EFFECT OF COUNTERWEIGHT FILL	LF.141
9.12	COUNTERWEIGHT FILL METHOD	LF.142
9.13	STEEL SHEET PILE METHOD	LF.143
9.14	VIBRO TAMPER METHOD	LF.144
10.1	LOCATION OF DAMAGED SITE AND LIQUEFIED AREA OF MAIN AGNO RIVER (1/3)	LF.145
10.2	LOCATION OF DAMAGED SITE AND LIQUEFIED AREA OF MAIN AGNO RIVER (2/3)	LF.146
10.3	LOCATION OF DAMAGED SITE AND LIQUEFIED AREA OF MAIN AGNO RIVER (3/3).....	LF.147

1. SUMMARY

(1) The magnitude of 16 th July 1990 Earthquake was 7.7 and the recurrent interval of this scale of earthquake is roughly estimated to be once in every 100 years in the study area. The ground acceleration was estimated to be 160 gal in Dagupan and 220 gal in the middle reach of Agno River.

(2) In Dagupan City the damage was concentrated in the area where the ground was once an ancient river channel, the reclaimed ground along the river and the area of past fish ponds, which are the same conditions pointed out by the case history study of liquefaction induced damage in Japan.

(3) In the middle to upstream reach of the Agno River, the damages were concentrated on the earth dikes. It is assessed that the heavily damaged dikes were caused mainly by the collapse of dike foundation, which in turn was induced mainly by liquefaction of the ground. The damaged shapes of earth dikes were characterized of sink, settlement of crest and slope, and longitudinal cracks on the crest and slope, and sometimes of swell, which are of similar nature as pointed out by the case history in Japan.

(4) The simplified prediction method which utilizes the SPT N value and the gradation analysis is used to determine the liquefaction of each 3 drilling holes in Dagupan and the middle Agno river.

It is supposed that the sand deposits in Dagupan City and in the middle Agno reach where liquefaction occurred mainly were in the shallow depth of 5 m to 8 m from the ground surface. The composite features of these sand deposits are mainly of fine sands which contain fine content (less than 75 microns) of 4 % to 33 %, mean particle size of 0.10 mm to 0.34 mm, specific gravity of 2.55 to 2.79, and gradation curves which are very similar to the sands liquefied by the Niigata Earthquake, 1964.

(5) The suitable countermeasures method against liquefaction for the earthdike are the shallow compaction method with a vibro tamper and the counterweight earthfill which is 4 m high and 12 m long from the toe of the dike slope in both land and river sides.

For the concrete revetment, the pile foundation and the soil improvement methods are the most effective.

(6) Further study for the earthquake and liquefaction in the study area should be carried out for the design of river structures.

2. OBJECTIVE

The earthquake was generated on 16th July 1990 during the feasibility study on the Agno River Basin. River and other structures were destroyed by this earthquake in the basin, Dagupan City area and other areas. The main cause of this damage is supposedly liquefaction.

Therefore, this liquefaction study has the following objectives.

- (1) To analyze the cause of the damaged river structures in the study area.
- (2) To analyze difference in liquefaction degree and to estimate the potential of liquefaction.
- (3) To research reference literatures concerning liquefaction and to study the possibility of liquefaction resistant design.
- (4) To predict roughly the risk of future liquefaction damage, and to provide necessary data for earthquake resistant design.

3. LIQUEFACTION PHENOMENA

3.1 General

It is understood that heavy damages on structures were attributable to liquefaction in the events of the Niigata and Alaska Earthquakes which were generated in 1964. Research on liquefaction was intensified since these earthquakes. Differential settlement of buildings, breakage of underground pipes, damage to roads and railways, and fall of bridges and river revetment occurred in the whole area of Niigata City during the earthquake. Large-scale landslides occurred in the Alaska Earthquake. Investigations conducted after the earthquake reveal that these were caused by the muddy water similar to fine sand emanating from the ground. Then, many studies with respect to the mechanics of its occurrence, prediction of earthquakes and countermeasures progressed. Most information in this chapter is adopted from YASUDA (1990), Ref. 1.

3.2 Earthquake Motion Causes Liquefaction

The released energy generated during an earthquake becomes the wave motion which propagate in the ground and reach to the ground surface. This wave motion contains the body wave (Primary wave and Secondary wave) that propagate in the elastic ground and the surface wave (Rayleigh wave and Love wave) that propagate in the vicinity of the boundary of the semi infinite elastic ground. The velocity of body wave is slower in the layer close to the ground surface, therefore the wave motion which occurred in this depth is refracted as shown in Fig. 3.1 and both the Primary wave (hereinafter P wave) and the Secondary wave (hereinafter S wave) propagate from just near the ground surface. The soil element of surface layer is acted by cyclic compressive and tensile force in vertical direction by the P wave as shown in Fig. 3.2 (a). The S wave adds to the cyclic shear force in horizontal direction as shown in Fig. 4.2 (b).

However, the shear force in the soil element does not occur when the lateral displacement of soil element is confined, because the lateral pressure $\Delta\sigma_3$ is mostly to be $\Delta\sigma_1$ when the compressive force of $\Delta\sigma_1$ is added to the soil element by the P wave. It is supposed that the influence by the P wave can be ignored, because the soil structure can resist

sufficiently against the isotropic pressure. Consequently there may be the problem that the soil behavior is affected by the S wave. The stress condition of surface wave is not clear and this wave is not adopted to the test and analysis of the liquefaction at present.

3.3 Liquefaction Mechanism Induced by Cyclic Shear

The soil element in some depth under the horizontal ground is taken notice as shown in Fig. 3.3 (a), provided that this soil is composed of sandy soil deposited loosely and below the underground water level (i.e. the void among the soil particles is saturated with water).

Before an earthquake, i.e. usually, the force acting among soil particles support the pressure which act on the upper part of soil element (overburden pressure of soil above the soil element, effective overburden pressure) and the pressure which act on horizontal direction σ'_{ho} as shown in Fig. 3.3 (b). The pore water occur only at static water pressure below the underground level. In this condition the shear strength of soil τ_f is expressed as follows:

$$\tau_f = C + \sigma' \tan \phi \quad (3.1)$$

where C = cohesion

ϕ = angle of internal friction

σ' = effective stress among soil particles

This strength can support the equivalent load of the structures. This soil element is acted by the cyclic shear during earthquake as shown in Fig. 3.3 (c) and (d), and destroyed of its particle structure (distribution). It is supposed that the soil is loose and the interlocking among the soil particles become loose gradually. This is caused by the negative dilatancy of granular material. The interlocking of soil particles become loose perfectly in the end as shown in Fig. 3.3 (e). This condition is same as muddy water that the soil particles are floating in the water. σ' becomes 0 in the equation (3.1), therefore $\tau_f = c$ which means shear stress 0 of sandy soil having no cohesion. This is the condition of perfect liquefaction. The pore water pressure should support the pressure of σ'_{vo} and σ'_{ho} which act round as before, and the pore water pressure overrise only the pressure of σ'_{vo} . (σ'_{ho} rise the value of

σ'_{vo} accompanied by the liquefaction, because it is understood that the soil element becomes the condition of liquid.)

It is necessary that the floating condition of soil particles in the water such as in Fig. 3.3 (e) is in the undrained condition which the pore water does not drain or in the little drain condition. The main earthquake motion continues to several scores seconds and it is usually supposed that the condition is perfectly undrained during this motion. However, the permeable ground like sandy gravel ground is considered of the drain effect.

The excess pore water pressure need to be dispersed after earthquake. The excess pore water seep to the horizontal ground surface. The seepage water, the liquefied sand and the soil in the ground spout at the same time, therefore the spouting hole and sand boil hill around its hole are formed. The appearance of Sand boil hole and hill will confirm the occurrence and location of liquefaction. According to witnesses, sand boil and fountain at the ground surface occurred a moment after the main earthquake motion.

For the seepage of excess pore water pressure observed in the model test on the shaking table, this excess pore water not only seep to the ground, but that it also seep rapidly through the crack in the ground and that just like boiling, it seep with stirring the soil particles. Accordingly it is supposed in two cases that the soil element stabilizes to be dense as shown in Fig. 3.3 (g) and that stirring makes soil particles deposit loose again after the dispersion of excess pore water pressure. Soil in the shallow depth which is stirred by the seepage water have the possibility of liquefaction occurring pattern (f).

The "reliquefaction" phenomenon is that the once liquefied ground liquefy again by the following earthquake. The ground in the case of (g) after earthquake is difficult to reliquefy and that in the case of (f) after earthquake is easy to reliquefy.

Fig. 3.4 shows the usual damage pattern induced by liquefaction on the ground and earth structures.

4. EARTHQUAKE

4.1 16 July 1990 Earthquake

The data of 16 July 1990 Luzon Earthquake are mainly compiled by the Philippine Institute of Volcanology and Seismology (PHIVOLCS). This earthquake was composed of two main shocks and many aftershocks. The first main shock was analyzed. The epicenter of this main shock is shown in Fig. 4.1. Isoseismal map of the first main shock is shown in Fig. 4.2 .

According to PHIVOLCS, the main records of the first main shock are as follows:

Date: July 16, 1990

Time: 4:26 PM 36.07 sec. (Philippine Time)

Duration: 45 sec.

Magnitude: Ms= 7.7 (USGS)

Location of epicenter: 13 km NNE from Cabanatuan

15.646 (0.025) N, 121.026 (0.052) E

Depth: 52.45 km (7.74 km)

Reported Intensity (on the Richter Scale), refer to Fig. 4.3

Int. VIII - Cabanatuan, Baguio, Dagupan, Tarlac

Int. VII - Manila

Int. VI - Quezon City

The second main shock occurred near Baguio City and caused the total damage of many buildings in Baguio. This second main shock has no detail data except the location. According to PHIVOLCS, this second one occurred about two (2) minutes after the first main shock and its magnitude was almost more than 7.0.

4.2 Recorded Earthquake in the Study Area

The epicenters of destructive earthquakes in the Philippines since 1589 to 1983 are 40. Instrumental determination of epicenters was applied during the period from 1911 to 1983. Epicenters before 1907 and in 1907

were located by using the respective Isoseismal maps.

These data show that the destructive earthquake occurred in 1786 (Int. X) and 1892 (Int. IX) around Dagupan City. In other words, the destructive inland earthquake has occurred once in almost every 100 years in the Study area. Other earthquakes in North Luzon Island that are considered not to cause total damages, has occurred every 10-15 years at the shortest.

According to the data of earthquake station in Dagupan City (from 1927 to 1987), earthquakes which have magnitudes of more than 6.0, occurred in 1927, '28, '32, '59, '61, '66 and '70. Earthquakes which have magnitudes of more than 7.0 occurred in 1966, 24 years ago. These data suggest that an earthquake which has a magnitude of more than 6.0 will occur at 1-2 years shortest interval and at 20 years longest interval, and an earthquake with a magnitude of more than 7.0 will occur at 25 -50 years interval. Earthquakes with magnitudes of more than 5.0 occurred almost several times in every year.

4.3 Fault

The fault which generated the 16 July 1990 earthquake is not the Philippine Fault Zone which runs through the Philippines for 1,000 km. The activity of Digdig Fault in north - west extended from the Philippine Fault Zone generated the 16 July 1990 earthquake (refer to Fig. 4.1). This Digdig Fault is supposed to be active in its length of about 150 km in the underground, and the left transverse displacement of about 100 km on the ground surface from Bongabon (NE of Cabanatuan), Puncan, Digdig to Mt. Pulog (40 km NE of Baguio) clearly occurred.

5. STUDY ON CASE HISTORY

5.1 Earthquake Damage of River Dikes (Ref. 4)

5.1.1 Damaged River Dikes by Past Earthquakes

The collected material of earthquake damage case history on river dike in Japan is shown in Fig. 5.1.

These earthquakes are as follows:

Earthquake Name	Year Generated
Nobi	1891
Kanto	1923
Fukui	1948
Tokachioki	1952
Niigata	1964
1968 Tokachioki	1968

The silty or clayey foundation also caused damage of river dyke due to settlement as shown in Fig. 5.1. The settlement by liquefaction of ground shows tendency to be larger than that of silty or clayey foundation.

5.1.2 Damaged Shapes of River Dikes

The damaged shapes of river dikes by earthquake are generally classified into 4 types as shown in Fig. 5.2.

Type I shows the slope surface failure on the embankment.

Type II shows the slope failure in the embankment.

Type III shows both the foundation and embankment failure.

Type IV shows the sink of embankment.

The Table 5.1 is to adopt the above shape classification for the case history as shown in Fig. 5.1, which shows the damage of Type II to be 1/3 and that of Type III and Type IV to be about 1/4 .

The damage of Types II, III and IV of river dike spoil the protecting

function for flood.

Fig. 5.3 shows how settlement occurred by damage shapes such as Types II, III and IV versus embankment height. The settlement shows the tendency to be large in proportion to the embankment height under the embankment height of 3-4m, however the settlement shows no increase beyond that height. In the range of the embankment height of 3-4m, the settlement of Type III shows about 3.7m and that of Type IV shows about 2.7m, while that of Type II shows about 2m. It is supposed that Type III failure along the sliding surface through the ground occur in case of liquefaction in the ground.

5.1.3 Ground under Heavily Damaged Dikes

It is pointed out frequently that the ground under the river dyke affects the earthquake damage occurring in the dyke. Especially, it is pointed out that closing dyke on the old river and dyke on the old river channel are heavily damaged.

5.2 Damage of River Structures by 1978 Miyagikenoki Earthquake (Ref.5)

5.2.1 Earthquake

The strong earthquake was generated in the Pacific Ocean in the vicinity of Miyagi-ken (Tohoku district) at 5:14 PM 12th June, 1978. The epicenter as shown in Fig. 5.4 was about 100 km from Miyagi-ken and its depth was about 30 km. The magnitude of this earthquake was supposed to be 7.4.

5.2.2 Outline of River, Topography and Geology

There are 7 first class rivers (decided by MOC in Japan) in Miyagiken and its total length is 284 km as shown in Fig.5.5. In general, the rivers flow from Ou Sanchi (mountainous district) in west to the Pacific Ocean in east. Upstream rivers are eroding the hilly area consisted of sedimentary soft rocks in Neogene period. Downstream rivers form the alluvial plain consisted of sand and sandy gravel.

The plain along the sea coast consist of unconsolidated sand and sandy gravel deposit, and under these deposits, are unconsolidated diluvial deposit and further Tertiary deposit in 30m to 60 m depth. There are backswamp of silt and clay deposit which form the soft ground behind natural levee at both river sides and shore levee along the shore-line.

5.2.3 Damage of River Structures

The damaged places and total length of river dyke, revetment, sluice pipe and weir are tabulated in Table 5.2. The location of damaged places of rivers are shown in Fig. 5.6. The number of location of damaged river dykes are 65 with a total length of about 19.5 km. The location of damaged revetment are 17 and its total length is about 1.4 km. The damage in each river is found much in the vicinity of the river mouth. For Yoshida River, the damage is also concentrated in the midstream about 14 km to 24 km from the mouth of the river.

(1) Damage of River Dike

The damage of river dike is summarized as below:

1) Dike Crest	Crack, Sink, Settlement
2) Berm	Crack, Sink
3) Slope	Crack, Swell, Failure
4) Special Dike	Displacement and Open of Joint Tilt of Parapet

The cracks are seen so many in the damage shapes and located at crest in mainly longitudinal direction as shown in Fig. 5.7. The cracks are found on the crest, berm and slope at the heavily damaged place, where sink occurred at the same time.

(2) Damage of Revetment

The characteristics of damage of revetment are as follows:

- 1) Masonry Revetment (6 places)
 - .Sliding failure of embankment slope
 - .Failure or collapse of revetment itself
- 2) Concrete Grillage Beam Revetment (11 places)
 - .Crack and breakage of lattice and slab
 - .Opening of joint between crest and slope
 - .Breakage by embankment sink and swell

(3) Sand Boil

The points where sand boil occurred are shown on Fig. 5.8. The characteristics of sand boil points are as follows:

- 1) Old River Channel (refer to Fig. 5.9)
 - Magaki (Kitakami R.), Wabuchi (Eai R.)
 - Fukuro (Yoshida R.), Arahama (Abukuma R.)
- 2) Crevasse
 - Yuriagekami dyke, Tanetsugi dyke (Natori R.)
- 3) Reclaimed Ground by Dredging
 - Kawamae (Kitakami R.)
- 4) There are many damaged dikes at the sand boil points or in the vicinity of these points.

5.2.4 Feature of Damaged Place

Generally speaking out from the past experiences of earthquakes, places which are easily and heavily damaged are as follows:

- a. Old River Channel
- b. Closing Dike of Old River
- c. Crevasse
- d. Soft Ground
- e. Newly Embanked Dyke
- f. Irregular Section connected by Access Road

Table 5.3 shows the damaged dikes to be classified as pointed out above. The above items from a to e are also unsafe points for flood and it is supposed that the weak points for flood will be also weak for the earthquake.

5.3 Settlement of Earth Structures Caused by the Nihonkai-Chubu Earthquake (Ref. 6)

5.3.1 Earthquake

The strong earthquake was generated in the Japan Sea in the vicinity of Akita-ken and Aomori-Ken (Tohoku district) on 26th May, 1983. The epicenter as shown in Fig. 5.10 was about 100 km from the boundary between Aomori-Ken and Akita-Ken. The magnitude of this earthquake was 7.7.

5.3.2 Outline of Damage

The damaged rivers total seven (7) as shown in Fig. 5.10. These rivers are the Iwaki R., Yoneshiro R., Omono R., Mogami R., Aka R., and Mabuchi R. It was especially Iwaki and Yoneshiro Rivers where damage was concentrated. The damage quantity of river dikes (including revetment is tabulated in Table 5.4.

5.3.3 Feature of Damaged Location

It is pointed out that the occurrence of earthquake damage on dyke is strongly affected by the epicenter distance and the quality of foundation ground. Fig. 5.11 shows the relation between the damage ratio of river dikes and the epicenter distance. This damage rate is obtained for each section of 10 km of its epicenter distance. It is clear from Fig. 5.11 that the damage of this earthquake occurred in the range of less than 160 km of the epicenter distance and the damage rate decrease with the epicenter distance becoming farther.

The relation as shown in Table 5.5 between damage and foundation ground is classified by micro-topography because there is almost no boring data regarding foundation ground of dikes. It is found in this table that reclaimed ground, old river channel and micro-high land of old river have relatively high damage rate. Soft silty, clayey or sandy soil are deposited in these ground in general. Consequently, it is supposed that the earthquake motion of foundation ground is amplified and further the low strength of ground during earthquake increase the damage rate of dike.

5.3.4 Liquefaction of Ground and Damage of Dike

One remarkable characteristic of this earthquake disaster is the liquefaction of ground. Table 5.6 shows the occurrence rate of sand boil, which is obtained from the ratio between the accumulated location number of sand boil occurring on the protected land of dyke and river side land in the range of scores m from dyke with the damaged locations number of dike by each river and micro-topography classification. It is distinguished that sand boils occurred in majority of all damaged locations. The occurrence rate of sand boil was very high on the old river channel and micro-highland of old river by the micro-topographic classification. The dyke damage on these grounds has a close relation with the liquefaction of ground.

The occurrence rate of sand boil in Iwaki River was very high because Iwaki River Basin is on the very gentle slope alluvial plain and the dikes are located mainly on the soft foundation ground as described in 5.3.3. Therefore, it is considered that the high damage rate of 5.1% as shown in Table 5.4 is caused by the above reason in spite of Iwaki River dyke being located relatively far, (about 140 km) from the epicenter.

5.4 Countermeasures against Liquefaction of Ground under River Dikes

The countermeasures adopted against the liquefaction of ground under the river structure in Japan in very few cases are stated below.

- (1) A compaction method was adopted for the closing dike of Shinano River by the sand compaction pile method.
- (2) A compaction method was adopted for the Ara River dike in Tokyo by the sand compaction pile method.
- (3) A partial replacement method was adopted for the ground near slope toe with unliquefiable soil after the Miyagikenoki Earthquake.

Natori River Yuriagekami dyke Tanetsugi dyke
Hirose River

- (4) A counterweight fill or a dynamic consolidation method were studied for the storm surge dike of 4 m high in Takase River, which flows from Ogawabara lake to the Pacific Ocean.

The details are described in the following sub section.

5.4.1 Countermeasures for Liquefaction Prevention of Reclaimed Ground (Ref 7)

(1) General

The Shinano River Closing Dyke (Niigata Pref.) is located on the loose sand ground which was reclaimed by dredging of river bed of Shinano River. (Fig. 5. 12). Therefore, on this ground is supposed that liquefaction will occur during an earthquake same as the Niigata Earthquake.

(2) Outline of Geology and Soil

The reclaimed soils under the closing dike are mainly loose fine sand to medium fine sand with a layer thickness of 10-12 m and its average N value is 3-5 in the whole area as shown in Fig. 5.13 .

The physical properties of this soil is as follows:

- 1) Fine particle content (under 0.074 mm) 1-70% average 15%
- 2) Coefficient of uniformity $U_c = 3-4$
- 3) Mean particle size $D_{50} = 0.2-0.5$ mm
- 4) Specific gravity $G_s = 2.65$
- 5) Relative density $D_r = 30-60\%$

(3) Study on Liquefaction

The laboratory cyclic triaxial test on the sample taken by the large size sampling was carried out and the result is shown in Fig. 5.14 and Fig. 5.15. Liquefaction is studied by the method of the simple judgment and the conclusion is summarized as follows:

- 1) The reclaimed sands under the closing dyke are the materials which are liquefiable.
- 2) This location is liquefiable for its topography and geology based on the past instances.
- 3) The records of generated earthquake in the past that were liquefiable in the vicinity of Niigata City, shows this ground has the potentiality of liquefaction.
- 4) This area has the potentiality of liquefaction up to about TP -10 m based on the instances during the Niigata Earthquake (equivalent to 0.162 g) and the calculation result.

(4) Countermeasures against Liquefaction

The countermeasures are selected from the following 4 methods of compaction as shown in Table 5.7 .

- 1) Sand Compaction Pile

- 2) Vibro Rod
- 3) Vibro Tamper
- 4) Vibro Flotation

The sand compaction pile method is selected because the ground contains finer particles more than 10%. The objective value of improvement judged by N value is a minimum of 10 and 13 on the average. The distribution of sand compaction pile of completed diameter 70 cm is the square and its pile interval is 1.7 m. The improvement range by the sand compaction pile is 70 m in width and 12 m in depth as shown in Fig. 5.16 .

(5) Field Trial Test

The SPT, vibration test in situ, undisturbed sampling and measurement of lateral K value are carried out prior to the construction of improvement.

The result is summarized as follows:

- 1) The N value after trial improvement is improved 13 number or more in the condition of finer particle content not exceeding 20% as shown in Fig. 5.17.
- 2) The N value which is 4 before improvement of finer particle content more than 20% is improved to about 8.
- 3) This improvement is shows that liquefaction will not occur compared with the Niigata Earthquake (about 160 gal) by the other information such as vibro test and lateral K value. It is judged that this condition of construction (pile diameter, pile interval and pile length) is suitable.

(6) Construction of Sand Compaction Pile

The construction of improvement is carried out on 6,400 m², about half of planned improvement area, and the quantity of piles is 2,193 (1=12m/pile). To determine improvement effect after construction, the SPT test is carried out. This frequency is one point per about 500 m² and 12 points are done.

The N values in B-2 and B-3 areas before and after the improvement are shown in shown in Fig. 5.18.

The improvement can attain its objective value (min. 10 and average 13) except for finer particles content $M > 60\%$. It is judged that the construction attained the objective that the improvement will be unliquefiable for the same magnitude as the Niigata Earthquake.

5.4.2 Countermeasures for Earth Dike of Natori River (Ref. 8)

The rehabilitation of the earth dike of Natori River which was fractured by the Miyagiken-Oki Earthquake was considered on the liquefaction countermeasures. The replacement method with crusherrun under 30 mm was adopted for the ground below the toe of the slope at the protected land side as shown in Fig. 5.19. The steel sheet piles were also installed into the ground below the toe of slope at the river side for the prevention of seepage.

5.4.3 A Study of Storm Surge Dike in Takase River (Ref. 9)

For the Takase River which flows from the Ogawabara lake to the Pacific Ocean in Aomori Pref., the storm surge dike 4 m high was planned to be made. The objective of this dike is also to prevent tsunami after earthquake. A sand boil was seen in the vicinity of this river during 1978 earthquake ($M=5.8$) which occurred just below this location. The detail liquefaction study was carried out and the total length of about 5 km was classified into 6 ground types. The soil investigation was made on the typical location, which were PS logging in the bore holes in situ, dynamic strength and dynamic deformation test in the laboratory.

The suitable established seismicity which was based on the investigation of seismic activity in the vicinity of this location was decided. The one dimensional seismic response analysis was carried out for the above 6 sections. The results of this analysis were compared with the liquefaction strength and the occurrence depth of liquefaction was predicted for each section as shown in Fig. 5.20. Further, the two dimensional seismic response analysis was carried out on the typical section and the distribution of FL (Liquefaction resistant factor, refer to Chapter 8) and

liquefiable range was obtained as shown in Fig. 5.21. The distribution of excessive pore water pressure was considered in carrying out the stability analysis.

The thick liquefiable layer in the sections was judged to be unstable. Therefore, several countermeasures against liquefaction were studied to compare with economical or other aspects and the compaction method by dynamic consolidation (refer to Section 9.1) or the counterweight embankment method were deemed adaptable. The effectiveness of these countermeasures were studied as shown in Fig. 5.22. The studied countermeasure range is shown in Fig. 5.22. and Fig. 5.23. The counterweight fill was seen to be installed farther than 6 m from the slope toe and the dynamic consolidation was needed to compact the soil depth up to 1.8 m from ground surface to obtain an N value about more than 15.

6 SITE RECONNAISSANCE

6.1 Dagupan City Area

The site reconnaissance was carried out in Dagupan City Area on 22nd to 24th January, 1991. Additional geological investigation was carried out as shown in Fig. 6.1 in Dagupan City.

The damages of these points and along the roads are described as follows:

(1) DG - 1

This boring point is in the site of Beer Ware House and this land was made of the reclaimed ground on the ancient river channel of the Pantal River as shown in Fig. 6.2. This figure was compiled by PHIVOLCS using the aerial photographs of the Dagupan City which were taken just after the Earthquake. The buildings in the site were damaged in the manner of settlement and tilt. The concrete slab of a parking area was heavily damaged as shown in Photo 6.1. The horizontal displacement might have occurred to the riverside at the same time the settlement occurred.

(2) DG - 2

This boring point was carried out near the damaged school as shown in Photo 6.2. This area was also made of the reclaimed ground as shown in Fig. 6.2. The concrete revetment of the Pantal River was destroyed by the earthquake as shown in Photo 6.3. The ground collapsed to the riverside. At the opposite side of the school, there is a church which was also damaged as shown in Photos 6.4 to 6.6. Bluish grey fine sand are seen in the cracks of the concrete slab of approach. The side walls of this church sank, hence the concrete slab of this church was bent except the center part.

(3) DG - 3

This point is in the vicinity of the fallen Magsaysay Bridge. The buildings around this point were heavily destroyed of their ground floor as

shown in Photo 6.7.

(4) DG - 4

This point has no damage.

(5) DG - 5

This point is behind the cinema and was made of the reclaimed ground on the former fish ponds. Settlement of about 40 - 50 cm occurred and this building was totally damaged as shown in Photo 6.8 and 6.9. The sand bags are piled to prevent the flood as shown in Photo 6.10.

(6) DG - 6

This point is the opposite site of the DG - 5. On the ground in the vicinity of this point occurred horizontal displacement and settlement. The concrete revetment of the Pantar River was deformed horizontally and vertically as shown in Photo 6.11.

(7) Angel B. Fernandez Avenue

The buildings along this avenue sank of about 40 to 50 cm in the east and about 20 to 30 cm in the west. Therefore, there are many totally damaged buildings as shown in Fig. 6.2 and as shown in Photos 6.12, 6.13 and 6.14. These photos show the level difference of the shop floor with the road. The damage is limited up to the intersection with Burgos Street.

(8) Dagupan - Lingayen Road (Perez Blvd.)

The damages of the buildings along this road were remarkably heavy as shown in Fig. 6.2 and in Photos 6.15, 6.16, 6.17 and 6.18. Settlement of about 1 m. occurred. Especially the north side buildings along this road were heavily damaged because this area is along the ancient river channel of the Pantar River. The features of damaged buildings are sinking and tilting as shown in Photo 6.15 and 6.16. The concrete pavement of a gasoline station was destroyed as shown in Photo 6.17. The hospital at the riverside in Photo 6.18 was constructed on a reclaimed land and its damage is a ground fracture.

(9) Magsaysay Bridge

Photos 6.18 and 6.19 show the fallen Magsaysay Bridge under rehabilitation. The 4 spans of this bridge fell due to the collapse of 2 piers and tilting of 1 pier as shown in Fig. 6.3.

(10) Site Inspection in September 1990

Site inspection by geological and physiographical view point was held from Sept. 12 to 18, 1990.

The following comments were obtained from the inhabitants along Angel Fernandez Avenue.

. The buildings sank down gradually at the beginning and then sudden settlement occurred by the biggest shock within 45 seconds of first main shock.

. At the same time, many cracks occurred along the road and sand boils were distinguished in the cracks. Most of the cracks ranged from 10 to 20 centimeters in width.

. The sand boils were composed of water and black sand which spouted about 20 centimeters high and this phenomenon lasted for about two or three minutes.

The following comments were obtained from inhabitants along Perez Boulevard Avenue.

. Big crack of about one meter occurred along the road at the beginning, and then closed at the last stage during the first main shock. Sand boils of 20-30 centimeters in height occurred along the cracks and this phenomenon lasted for about 1 minute. A mother and her child fell down in the crack, however, they were rescued after the main shock.

. Building settlement gradually occurred at the beginning and the building suddenly sank down with the biggest shock during the first main shock. Sand boils were recognized along the cracks on the ground.

. The heavily damaged areas along the southern main road were former fish pond many years ago and filled up as development of Dagupan City takes shape. Non-damaged area was the same circumstance as before.

The information from the Geological Survey Division of BMG* are as follows:

- 1) The area along the existing river and old channel were filled up with sandy materials, clay and gravel including much sawdust. Infill material with sawdust are not enough foundation for buildings.
- 2) Many buildings have no piling for their foundation except one six storey hotel which was not damaged.
- 3) Non-damaged buildings were mostly Spanish type ones built long before. Therefore, these areas are considered to be neither river bed nor an old river channel.
- 4) The heavily damaged buildings exist almost along the existing river and old channels, and those areas were filled up with infill materials described above.

* Bureau of Mines and Geo - Sciences, Department of Environment and Natural Resources

6.2 Middle Agno River

In the Agno River Basin the heavily damaged structures, mainly earth dikes are concentrated in the midstream basin. Figs. 6.4 and 6.5 show the location of damaged sites, the additional and original boring points. The site reconnaissance was carried out on 23rd and 24th of January, 1991 in the middle Agno River.

The damage of these sites from upstream side are described as follows:

(1) MA 1 (Santa Maria - Tayug Earthdike)

The crest of earth dike sunk and many cracks occurred as shown in Photo 6.20 . This portion of dike was fractured when the flood after the earthquake washed away the dike as shown in Photo 6.21.

(2) MA 2 (Santa Maria - Tayug Earthdike)

The crest of earth dike sunk about 1.5 m - 2.0 m and many longitudinal cracks along the dike occurred on the crest and slope as shown in Photos 6.22 and 6.23. Fig. 6.6 shows the profile along the center and the cross section of damaged earthdike. The vertical displacement occurred at the boundary between firm and soft ground as shown in Photo 6.24. In Photo 6. 23 the sand boil from the well (steel pipe of about 10 cm diameter) is seen at the protected land side.

(3) Villasis - Asingan Earthdike (AG 364 - AG 365 to AG 368 - AG 369)

This earth dike with a total length of 2 km is already reconstructed as shown in Photo 6.25. There are many ponds or marshes in the vicinity of the dike at the protected land side.

(4) Asingan Revetment of Concrete Dike (AG 368 - AG 369 to AG 369 - AG 402)

This concrete revetment has damaged feature of breakage by vertical displacement as shown in Photo 6.26. There is likewise the settlement of crest where many cracks occurred as shown in Photo 6.27.

(5) MA 3 (Bayambang - Villasis Earthdike)

This site has damaged crest where cracks occurred. This dike was also breached by the flood after the earthquake which washed away almost half of its cross section as shown in Photo 6.28 and 6.29.

(6) MA 4 (Alcala - Santo Tomas Earthdike)

The dike crest sunk down of about 1.5 - 2.0 m and longitudinal cracks

occurred at the shoulder of slope as shown in Photo 6.30.

(7) MA 5 (Alcala - Santo Tomas Earthdike)

This dike site heavy damage is mostly collapsed embankment that might have occurred with the ground failure as shown in Photo 6.31 and 6.32.

(8) MA 6 (Bayambang - Villasis Earthdike)

This dike with a length about 9 km is already reconstructed in most sections as shown in Photo 6.33. Fig. 6.7 shows the profile along the center and the cross section of damaged earthdike. MA 6 point is located near marsh as shown in Photo 6.34. Photo 6.35 shows rehabilitated section washed away due to dike fracture by flood.

(9) MA 7 (Bayambang Stretch of Concrete Dike)

The parapet of this dike was destroyed at two locations and total damaged length is about 100 m as shown in Photo 6.36. Many cracks occurred in the whole length of 1.9 km.

(10) MA 8 (Poponto Floodway, Right Earthdike)

Longitudinal cracks occurred on the slope and there is settlement of crest about 1.0 m as shown in Photo 6.37. Photo 6.38 shows the boring location of MA 8.

(11) MA 9 (Bautista - Anulid Earthdike)

This dike sunk and was destroyed heavily. Cracks occurred on the crest and slope. The settlement is about 1.7 - 1.8 m. to a maximum of 3.0 m. Photos 6.39 and 6.40 show the damage of this dike and photo 6.41 shows the location of boring point.

(12) MA 10 (Riverside in Nanambong)

This vertical displacement of about 2 m - 2.5 m maximum occurred as shown in Photo 6.42. However, this displacement was reduced further to

about 1 m due to the flood after the earthquake. Severe settlement occurred for about 500 m of the 2 km. total length that was transformed in straight direction. Many cracks and small displacements were observed. These findings were obtained during the site inspection conducted in September 1990. Sand boils of 1 m in height were obviously recognized by the inhabitants and this phenomenon lasted continuously for about 30 minutes.

The spouted fine sand in the field are seen around the well (steel pipe of about 10 cm diameter) in the vicinity of MA 10.

(13) Sison Bridge (Carmen)

The 6 spans of the simple steel truss superstructure where consisting of 13 spans (total length 655 m) fell at the left side over the Agno River because the 5 piers tilted to the river direction as shown in Fig. 6.8. Photos 6.43, 6.44 and 6.45 show the damaged Carmen Bridge. Sand boils were identified near the bridge after the earthquake.

(14) Calvo Bridge (Bayambang)

This bridge consisted of 4 spans simple steel truss each 50 m long. The P1 pier at the left side tilted to the river direction and 2 spans of steel truss fell as shown in Photo 6.46 and in Fig. 6.9.

(15) Upper Agno River near Santa Maria

The site inspection conducted in September 1990 had resulted in clear evidence of sand boil near Santa Maria. The spouted gray medium sand, remained still on the ground of river side of Upper Agno River. Sand boils lasted for about 40 to 50 minutes. The cracks observed in the site showed that its length was about 300 m, its width was 60 to 80 cm and its depth was 60 to 80 cm. The depth of cracks might have reached 2 to 2.5 m just after the earthquake.

7. FIELD INVESTIGATION AND LABORATORY TEST

7.1 Method

The objective of this investigation is to obtain the necessary data utilizing the bore hole of the additional foundation investigation. Consequently, the 6 borings, 3 holes in Dagupan City Area (refer to Fig. 7.1) and 3 holes in the middle Agno River (refer to Figs. 7.2 and 7.3), were replaced with the core borings of 100 mm diameter, carried out by the standard penetration test (hereinafter called SPT) with 1.0 m interval and by the core tube sampling. The core tube and SPT samples obtained from each boring were sent to the laboratory and test were carried out. The quantity of these borings and laboratory tests are tabulated in Table 7.1. Field density tests to measure the SPT sample were done. However, reasonable results could not be obtained so these were omitted.

7.2 Site Geology

7.2.1 Dagupan City

The thickness of surface soil which is composed of the fill material is about 1.5 m to 5 m in the Dagupan City Area. Fine sand or fine to medium sand deposits are existing under the surface soil. The silt or clay layer is seen at 18.45 m depth in DG-1, at 15.0 m depth in DG-3 and at 12.0 m depth in DG-5.

The detail of each bore hole is shown in Figs. 7.4 to 7.6 and described as follows: (The legend of bore hole should be referred to Fig. 7.10)

(1) DG - 1 (refer to Fig. 7.4)

This location consisted of reclaimed land along the Pantar River. The surface layer of 2 m deep consists of silty and sandy clay. The deposit from 2.0 m to 18.45 m deep is composed of mainly loose fine sand, N value: 2 to 10, except the depth of 5 m - 7 m and 13 m - 16 m (N value: 17 to 23). The deposit under 18.45 m deep is composed of stiff to soft dark grey silty clay.

(2) DG - 3 (refer to Fig. 7.5)

The surface layer 5 m thick consists of very loose silty sand and fine sand. The deposit up to 8 m deep consists of loose fine sand (N value: 5 to 7). The deposit from 8 m to 16.45 m deep consists of medium dense fine sand with N value of 23 to 33 except the thin clayey silt layer. The underlying deposit of grey silty and sandy clay is stiff.

(3) DG - 5 (refer to Fig. 7.6)

This location was filled on a former fish pond. The 5 m thick fill consists of very loose gravelly sand and very fine sand. The underlying deposit up to 12 m deep consists of dark grey fine sand with N value showing 23 to 34, medium dense, except N = 6 (depth 5.15 - 5.45 m) and N = 70 (depth 10.15 - 10.45 m). The deposit which is under 12 m deep consists of hard dark grey clayey silt and sandy silt up to 16 m deep. The dark grey sandy silt under 16 m deep is stiff.

7.2.2 Middle Agno River

Three (3) boring points were decided to be undertaken to investigate the cause of dike fracture in the middle Agno River. The detail of each bore hole is shown in Figs. 7.7 to 7.9 and described as follows:

(1) MA - 2 (refer to Fig. 7.7)

The embankment material of earth dike is same as the ground foundation of dike. The dike and ground up to 5.45 m deep consist of hard to stiff brown sandy silt. The underlying dark brown clayey sand and grey fine to medium sand are medium dense, which N value is 17 and 18. The deposit under 10 m deep consists of grayish gravel and sand mixture up to 15 m deep, and grayish brown and light grey gravel sand mixture with cobbles up to 20 m deep. It is supposed that these gravel sand mixtures are dense.

(2) MA - 5 (refer to Fig. 7.8)

The embankment material of earth dike is same as the foundation ground

of dike. The brown fine sand with silt consists of loose ground which N value is 6 to 9 in the depth of 5 m . The deposit in 5 m to 8 m deep consists of grey to dark grey, fine to coarse sand which are loose (N value : 13) to medium dense (N value: 35). The underlying deposit under 8 m deep consists of grey to brownish grey, fine to medium sand which is medium dense to dense of N value from 22 to 39 except 14 (depth 18.15 - 18.45 m).

(3) MA - 6 (refer to Fig. 7.9)

The surface layer is only 32 cm thick and soft brown clayey silt. The deposit up to 2.45 m deep is loose brown to brownish grey silt sand (N value : 10). The deposit from 2.45 m to 6.0 m deep consists of loose grey fine to medium sand which N value is 6 and 15. The underlying grey silty clay forms soft to hard layer from 6.0 m to 9.45 m in depth. The deposit under 9.45 m deep consists of medium dense (N value: 19 to 32) to dense (N value: 41 to 61), brownish grey to grey and fine to medium sand.

7.3 Laboratory Test

The summary of laboratory test results are tabulated in Tables 7.2 and 7.3. The features of soils are described. For liquefaction analysis, the gradation of soils is very important.

7.3.1 Dagupan City

The fines content (under 0.074 mm, silt and clay) of fine to medium sands is minimum 4% to maximum 33% and 17% on the average. The mean particle size D range within 0.10 mm to 0.34 mm. The natural moisture content of sands range from 11% to 37%. These atterberg limits of sands except DG - 5 (depth 2.15 m - 2.45 m) are non plastic. The specific gravity of these sands have a little wide range of 2.59 to 2.79.

The plasticity index of silty clay under 18.45 m in depth of DG -1 is 8. The plasticity index of silty clay and sandy clay under 16.45 m of DG - 3 is 17 and 10 respectively. The physical property of clayey silt under 12.0 m in depth of DG - 5 is 44% of natural moisture content, 15 of plasticity index and 2.56 of specific gravity. The underlying sandy silt layer has the variant plasticity index of 6, 18 and 11.

7.3.2 Middle Agno River

The fines content of fine to medium and coarse sands is minimum 6% to maximum 31% and 17% on the average. The mean particle size D range within 0.11 mm to 0.31 mm. The natural moisture content of sands ranges from 11% to 34%. These atterberg limits of sands except MA - 2 (depth 6.0 m - 7.0 m) and MA - 6 (depth 5.0 m - 6.0 m) are mostly non plastic. The specific gravity of these sands have a little range of 2.55 to 2.77.

The physical properties of gravel sand mixture under 10 m up to 15 m of MA - 2 are 6.3 mm of D^{50} , 19% of natural moisture content and 2.66 of specific gravity. The plasticity index of upper sandy silt of MA - 2 is 5 and 10. The plasticity index of middle silty clay layer (6.0 m to 9.45 m) of MA - 6 is 29 and 26.

7.3.3 Feature of Sand Deposit

The feature of sand deposit is summarized in Table 7.4

The gradation curves in each bore hole are shown in Fig. 7.11 to Fig. 7.16 respectively.

The average fines content of each bore hole is as follows:

Boring No.	Average Fines Content (%)
DG - 1	18
DG - 3	17
DG - 5	16
MA - 2	20
MA - 5	18
MA - 6	14

Fig. 7.17 shows the range of gradation curves of sand deposits in Dagupan and middle Agno reach, and this figure also shows the range of gradation curves of sand boil which spouted during and after the Niigata Earthquake. The whole range of gradation curves of deposit sands in Dagupan and middle Agno reach contain a little finer particles than spouted sands by the Niigata Earthquake. However, this range is very similar to the range of gradation curves of sand boil in Niigata Earthquake. This figure suggests that the sands mainly consist of fine sands finer than 0.425 mm.

The gradation curve of river sand taken in middle Agno reach, near Asingan is shown in Fig. 7.18 for reference. The coefficient of uniformity and curvature of sand deposits only obtained in D10 are $U_c = 2.0 - 3.8$ and $U_c' = 0.8 - 1.5$ respectively shown in Table 7.5 except for MA-2 (12.0 m - 13.0 m).

8. ANALYSIS OF LIQUEFACTION

8.1 Methodology

The analysis of liquefaction is carried out using the simple prediction method which utilizes the SPT N value and the gradation of soil. This method is commonly used in Japan to determine the liquefaction in soil deposits. An up-to-date Specifications for Highway Bridges (PART V, Earthquake Resistant Design) edited in 1990, Japan Road Association, is the most advanced and widely used method in Japan. This flow of liquefaction analysis is shown in Fig. 8.1.

8.1.1 Liquefaction Resistant Factor

Liquefaction resistant factor FL is defined in the following equation (8.1) and this value if not exceeding 1.0 is judged to be liquefiable.

$$FL = \frac{R}{L} \quad (8.1)$$

where, R : Strength ratio causing liquefaction or
Dynamic Shear Strength Ratio

L :Cyclic shear stress ratio induced by earthquake

L is expressed in the following equation (8.2).

$$L = rd \cdot ks \cdot \frac{\sigma_v}{\sigma_v'} \quad (8.2)$$

where, rd : Reduction factor for depth

ks : Seismic coefficient at ground surface

σ_v : Overburden pressure (kgf/cm²)

$\sigma v'$: Effective overburden pressure (kgf/cm²)
 r_d : 1.0 - 0.015z (8.3)

z : Depth from ground surface (m)

k_s : α_{max}/g (8.4)

α_{max} : Maximum ground acceleration (cm/sec²)

g : Gravity acceleration (cm/sec²)

σv : $\{\rho_{th} + \rho_{sat}(z-h)\} / 10$ (kgf/cm²) (8.5)

$\sigma v'$: $\{\rho_{th} + (\rho_{sat} - 1.0)(z-h)\} / 10$ (kgf/cm²) (8.6)

ρ_t : Wet density of soil (tf/m³)

ρ_{sat} : Saturated density of soil (tf/m³)

h : Depth of ground water level (m)

R is expressed in the following equation (8.7).

$R = R_1 + R_2 + R_3$ (8.7)

where, $R_1 = 0.0882 \frac{N}{\sqrt{\sigma v' + 0.7}}$ (8.8)

N : SPT N value

$R_2 = \begin{cases} 0.19 & (0.02\text{mm} < D_{50} < 0.05\text{mm}) \\ 0.225 \log_{10} (0.35/D_{50}) & (0.05\text{mm} < D_{50} < 0.6\text{mm}) \\ -0.05 & (0.6\text{mm} < D_{50} < 2.0\text{mm}) \end{cases}$ (8.9)

D50 = Mean particle size (mm)

$$R3 = \left\{ \begin{array}{ll} 0.0 & (0\% < Fc < 40\%) \\ 0.004FC - 0.16 & (40\% < Fc < 100\%) \end{array} \right\} \quad (8.10)$$

Fc : Fines content (%)

In these equations R1 is expressed with the function of N value and effective overburden pressure σ_v' , R2 is expressed with the function of mean particle size D50, and R3 is expressed with the function of fines content FC.

8.1.2. Established Seismic Coefficient

The next equation for calculating ground acceleration is obtained based on the SMAC type (strong motion accelerometer) records of horizontal 394 components by 88 earthquakes in Japan, which is proposed by the Public Works Research Institute of MOC in Japan.

$$\alpha_{\max} = 232.5 \times 10^{0.313M - 1.218} \times (\Delta + 30)$$

where, α_{\max} : Maximum ground acceleration

M : Magnitude of earthquake

Δ : Distance from epicenter (km)

The magnitude of North Luzon Earthquake was 7.7.

The distances from epicenter of Dagupan City and the middle Agno reach are about 100km and 70km respectively as shown in Fig. 8.2. Therefore, the maximum ground acceleration and k_s (equation 8.4) are calculated as follows:

o Dagupan City

$$\alpha_{\max} = 232.5 \times 10 \left(\frac{0.313 \times 7.7}{-1.218} \right) \times (100 + 30)$$

$$= 232.5 \times 10 \left(\frac{2.4101}{-1.218} \right) \times 130$$

$$= 232.5 \times 257.1 \times 0.00266$$

$$= 159 \text{ gal}$$

$$k_s = \alpha_{\max} / g = 159 \text{ cm/sec}^2 / 980 \text{ cm/sec}^2 = 0.16$$

o Middle Agno Reach

$$\alpha_{\max} = 232.5 \times 10 \left(\frac{0.313 \times 7.7}{-1.218} \right) \times (70 + 30)$$

$$= 232.5 \times 10 \left(\frac{2.4101}{-1.218} \right) \times 100$$

$$= 232.5 \times 257.1 \times 0.0037$$

$$= 221 \text{ gal}$$

$$k_s = \alpha_{\max} / g = 221 \text{ cm/sec}^2 / 980 \text{ cm/sec}^2 = 0.226$$

8.2 Calculation of Liquefaction

The liquefaction resistant factor is affected by the following factors.

- 1) Ground water level
- 2) Density of each layer
- 3) Established seismic coefficient

In July 1990, the ground water level of each bore hole is assumed to be the same level of ground surface or less because it was rainy season in

Dagupan City and the middle Agno reach and it is supposed that the ground water level was close to the ground surface at each location.

The density of each layer could not be measured, consequently the wet and saturated density were referred to Table 8.1 in the specifications for Highway Bridges, PART V, Earthquake Resistant Design, 1990.

The seismic coefficient is established in the subsection 8.1.2.

This liquefaction resistant factor FL can be adopted only for the horizontal ground, therefore, this is calculated on the horizontal ground in the vicinity of river dike for bore holes MA-2 and MA-5. The calculation of FL for each bore hole is carried out according to equation 8.1 and the results are shown in Figs. 8.3 to 8.8.

8.3 Evaluation on Liquefaction

According to the calculation results of liquefaction (8.2), the liquefied layer of 16th July 1990 Earthquake in each bore hole is determined and shown in Figs. 8.9 to 8.14. It is supposed that the liquefied layer in the Dagupan City occurred in shallow depth 5m to 8m from ground surface except 7.3 m to 12.1 m in DG-1 and that in the middle Agno reach, it also occurred mainly in shallow depth 5 m to 8 m from ground surface as shown in Table 8.2. The liquefied layers of MA-5 and MA-6 deeper than 10 m from the ground surface are thin except from 15.0 m to 18.4 m in MA-6. The shallow depth of liquefied layer in Dagupan City and the middle Agno reach resulted to heavy damage to the buildings, structures and river earth dikes induced by the ground fracture.

9. COUNTERMEASURES AGAINST LIQUEFACTION FOR RIVER STRUCTURES

9.1 Basic Concept

The basic countermeasure to prevent damage is shown in Fig. 3.4 (b) or described in Chapter 6. The river structures are classified into two structure types. One is earth dike and another is concrete revetment. The countermeasure methods against liquefaction for the existing earth dike are described as follows;

- 1) Increase the density of ground with compaction
- 2) Replace the loose sand with good materials such as crusherrun or gravel
- 3) Mix and stir the loose sand with cement milk by machine
- 4) Place the counterweight fill to increase the effective overburden pressure
- 5) Install the gravel drain pile in the ground
- 6) Confine the deformation of ground with steel sheet pile and steel rod or cable.

These methods are tabulated in Table 9.1 and compared with their merits and demerits.

The outline of these methods are shown in the following figure.

Sand compaction Pile	Fig. 9.1
Rod Compaction	Fig. 9.2
Dynamic Consolidation	Fig. 9.3
Deep Mixing	Fig. 9.4
Gravel Pile	Fig. 9.5

In these methods, rod compaction should be eliminated because ground under earth dike contain fines content (finer than 0.074 mm, silt and clay) more than 20%. The replacement method also should be eliminated because the supposed liquefied deposits exist deeper than 5 m and the stability of dike during excavation is supposed to be unsafe. Furthermore, the ground water level is shallow and temporary sheet piles should be used to excavate the ground for safety and cut-off.

The gravel drain pile should be used together with another countermeasure method and should not be adopted singly.

Therefore, other 5 methods are further compared in Section 9.2.

The suitable countermeasure method against liquefaction for the concrete revetment is the pile foundation (PC pile, steel pipe pile, etc.) which should be considered on liquefiable layer to reduce the resistance of this layer. Other method is soil improvement as shown in Table 9.1.

9.2 Selection of Countermeasures

The typical section chosen to be studied on liquefaction is MA-5 in the middle Agno reach because its log consists of mostly sandy soils and FL values are smaller than other 2 holes.

The countermeasures against liquefaction for the ground are adopted to the shallow portion up to 8 m from the surface. It is very effective to avoid liquefaction on the shallow ground, where ground failure will not occur.

9.2.1 Sand Compaction Pile

The sand compaction pile (hereinafter SCP) is driven on both grounds of the protected land and riversides as shown in Fig. 9.7. Chart (a) of Fig. 9.6 shows the relationship between improvement ratio (F_v) and increase in N-value as follows:

No	N1
6	15
9	19
13	23

where, No : N value before improvement

N1 : N value after improvement

Improvement ratio of $a_s = 0.10$ means the interval of sand piles of about 2.0 m as shown in Fig. 9.7. According to the N value after improvement, the FL values are 1.0, 1.11 and 1.18 respectively.

The seismic coefficient is supposed to be 0.20 as noted from similar experience in Japan. However, this coefficient should be studied further in detail design stage. This SCP method affects much vibration to the ground and existing structures.

9.2.2 Dynamic Consolidation

This dynamic consolidation is applied on the ground of both sides of existing earth dike. Fig. 9.8 shows the increasing N value by tamping energy. According to this figure, E_v is equivalent from a range of 38 to 94 m and the increased N value is estimated from a range of 10 to 20 for $D = 5.3$ m. The N values in the shallow ground, 6, 9, 13 are supposed to increase to 16, 19 and 23 respectively. The improved FL values are 1.03, 1.11 and 1.18 provided that seismic coefficient is supposedly 0.20. This dynamic consolidation method affect much vibration to the ground and existing earth dike. The tamping area of the ground is shown in Fig. 9.9. The effectiveness in shallow portion of ground (0m - 2m) is less than in middle or deep portion. Therefore, recompaction on ground is required after tamping with other machines.

9.2.3 Deep Mixing

The slurry type which uses the stabilizer of cement milk or mortar is suitable deep mixing method for protecting liquefaction of sandy ground. The improvement ratio of about 100% should be applied in the improved ground. This deep mixing method is shown in Fig. 9.10.

9.2.4 Counterweight Fill

The counterweight fill on the liquefiable ground at both sides of earth dike is effective to increase the overburden pressure of ground and protect from sliding of dike slope. Fig. 9.11 shows the effect of this counterweight fill of 4 m high and 12 m long that increases mostly the FL value more than 1.0, provided that seismic coefficient is supposed to be

0.20. The applied section to earth dike is shown in Fig. 9.12. However, liquefaction under the toe of the counterweight fill can not be avoided with this method.

9.2.5 Steel Sheet Pile

This steel sheet pile method aims to confine the deformation of earth dike; however, it is very difficult to estimate the effectiveness quantitatively. The end of sheet pile should be driven into the medium dense sand layer or stiff clay layer. The top of sheet piles should be joined with steel C channels and a tie rod or cable is used to unite both sides of sheet pile. Fig. 9.13 shows this method.

9.2.6 Comparison of Cost

The direct cost per 1 m of earth dike on countermeasure methods are compared in Table 9.2. These unit costs which are commonly used in Japan are applied. However, the unit cost of these soil improvement methods in the Philippines; SCP, Dynamic Consolidation and Deep Mixing, is supposed to be twice compared with the unit cost in Japan.

9.3 Recommended Countermeasure

The counterweight fill is the most economical method as shown in Table 9.2. This method does not affect the earth dike and easy to construct in the Philippines. Land acquisition at both sides of dike should be required at more than 12 m. If the earth dike will collapse due to earthquake, the rehabilitation will be carried out soon using the counterweight fill. In the shallow ground up to 3 m deep, unsuitable layer exists and this layer should be improved with other suitable methods. One of these methods, the vibro tamper method, can improve the shallow ground up to 3 m with compaction by the tamper (2 m x 2 m) which is connected to a vibrohammer hung by crawler crane as shown in Fig. 9.14. The direct cost of this method in Japan is 700 yen per 1 m².

10. CONCLUSION AND RECOMMENDATION

10.1 Conclusion

(1) The magnitude of 16th July 1990 Earthquake was 7.7 (PHIVOLCS) and the epicenter of this earthquake was 16 km NNE from Cabanatuan and near the town of Bongabon as shown in Fig. 8.2. The seismic intensity in the Study Area (Dagupan-Rosales area) is reported to be VIII on the Richter Scale. The recurrent interval of this scale of earthquake is roughly estimated to be once in every 100 years in the study area.

(2) A case history of the liquefaction induced damage in Japan has been studied and the following facts have been identified:

- a) The dike damage is classified to be crack, sink, settlement and swell,
- b) The damaged shape of river dikes by liquefaction is classified to be the type III as shown in Fig. 5.2 with both foundation and embankment failures,
- c) The features of heavily damaged places and facilities were ancient river channels, closing dikes or weirs for the ancient rivers, crevasses of dikes, soft silty or clayey ground, newly embanked dikes and dikes having irregular sections.
- d) Sand boils occurred in such places as ancient river channels, crevasses of dikes and reclaimed lands by dredging.

(3) The following observation was obtained from site reconnaissance.

- a) In Dagupan City, the damage was concentrated in the area where ground was once an ancient river channel, the reclaimed ground along the river and the area of past fish ponds as shown in Fig. 6.2. The primal cause of these damage was assessed to be liquefaction of ground as evidenced by sand boils.
- b) In the middle to upstream reach of the Agno River the damages were concentrated on the earth dikes. The sink and settlement of the major dikes were in the range of 0.2 m to 2.0 m. Longitudinal cracks were mainly observed on the crest and slope of earthdikes as shown in

Figs. 6.6 and 6.7.

It is assessed that the heavy damage on dikes were caused mainly by the collapse of dike foundation. Foundation collapse is supposed to be induced mainly by liquefaction of the ground.

(4) The field investigation result of each 3 drill holes in Dagupan and middle Agno reach and the succeeding laboratory tests reveal the property of ground and sands as follows:

- a) The thickness of surface soil which is composed of the fill material is about 1.5 m to 5 m in Dagupan City. Fine sand or fine to medium sand deposits are existing under the surface soil. The silt or clay layer is seen at 18.45 m depth in DG-1, at 15.0 m depth in DG-3 and at 12.0 m depth in DG-5 . These are shown in Figs. 7.4 to 7.6. The ground water level in each hole was shallow.
- b) In the middle Agno reach the MA-2 shows sandy silt of 3 m thick and medium dense silty sand up to 10 m as shown in Fig. 7.7. There are dense sandy gravel under these layers. MA-5 is composed of loose silty sand up to 6 m and dense or medium dense silty sand continued up to 20 m as shown in Fig. 7.8. MA-6 is composed of loose silty sand up to 6 m and stiff or hard silty clay layers of about 4 m and dense or medium dense silty sand continued as shown in Fig. 7.9. The ground water level in each hole was shallow.
- c) The physical property of the sand deposits is shown in Tables 7.2, 7.3 and 7.4 and is summarized as follows;

The fines content range from 4% to 33% (average 17%).

The mean particle size is 0.10 mm to 0.34 mm.

The specific gravity is 2.55 to 2.79.

The gradation curves are very similar to the sands liquefied during and after Niigata Earthquake as shown in Fig. 7.17. These sands are mainly composed of fine sand.

(5) Liquefaction analysis for each drill hole is carried out based on the specifications for Highway Bridges, PART V, Earthquake Resistant Design method edited in 1990 in Japan. The result is described as follows:

a) The induced ground acceleration by 16th July 1990 Earthquake in Dagupan is assessed to be about 160 gal and that in the middle Agno reach is assessed to be about 220 gal.

b) The simple prediction method which utilizes the N value (SPT) and the gradation analysis is used to judge the liquefaction. According to the calculation result for liquefaction, the liquefied layer in Dagupan City occurred mainly in the shallow depth of 5 m to 8 m from the ground surface and that in the middle Agno reach, it also occurred mainly in the shallow depth of 5 m to 8 m from the ground surface. These liquefied layers are shown in Fig. 8.8 to Fig. 8.13.

(6) It is assessed that the damaged river structures were affected by the their ground fracture which were induced by liquefaction (refer to Figs. 10.1 to 10.3).

(7) The countermeasure practices against liquefaction for river structures in Japan were few. These are sand compaction piles, a partial replacement method and a counterweight fill or a dynamic consolidation method.

The study on the countermeasures against liquefaction is carried out and the conclusion is as follows;

a) The suitable method for the earth dike is the shallow compaction with the vibro tamper and the counterweight fill which is composed of an earthfill 4 m high and 12 m long in the toe of the dike slope in both land and river sides.

b) The suitable method for the concrete revetment is the pile foundation which should be considered on liquefied layer to bear the difference of reduced resistance of this layer. Another method is soil improvement method as shown in Table 9.1.

c) The unit cost of these soil improvement methods in the Philippines is supposed to be twice compared with the unit cost in Japan.

10.2 Recommendation

(1) The historical earthquakes in the Philippines and the study area shall be further studied to provide information required for design.

(2) It is recommended to provide countermeasures against liquefaction in case of earth dike construction.

11. REFERENCES

- 1) Susumu Yasuda : From Investigation to countermeasure of Liquefaction, 1990 Kajima Shuppankai
- 2) Department of Science and Technology, PHILIPPINE INSTITUTE OF VOLCANOLOGY AND SEISMOLOGY
- 3) Tokuji Utsu : Dictionary of Earthquake, 1987, Asakura Shoten
- 4) Yasushi Sasaki : Earthquake Damage of River Dikes
Tsuchi to Kiso (Soils and Foundation) PP25-30 August, 1980
- 5) Takashi Kawakami, Yasuo Watanabe : Damage of River Structures by 1978 Miyagiken-Oki Earthquake
Technical Study Report in MOC Vol. 32 1978 PP589-595
- 6) Yasushi Sasaki, Eiichi Taniguchi, Osamu Matsuo, Yoshihiro Ito:
Settlement of Earth Structures caused by the Nihonkai-Chubu
Earthquake, Tsuchi to Kiso (Soils and Foundation) PP7-13 September, 1984
- 7) Teiichi Ishida, Goro Takahashi : Countermeasures for Liquefaction
Prevention of Reclaimed Ground
Technical Study Report in MOC Vol. 31 1978 PP77-83
- 8) Kyoza Suga, Yasushi Sasaki, Yukitake Shioi : Damage of River Dikes,
Report on the Disaster Caused by the Miyagiken-oki Earthquake of
1978, Report of Public Works Research Institute in MOC, Vol. 159 PP189-
190 March, 1983
- 9) Yasushi Sasaki, Zenji Sawada, Susumu Yasuda, Yutaka Tanoue:
A Study of the Stability of Takase Bank during an Earthquake, Tsuchi to
Kiso (Soils and Foundation), PP19-24, August, 1987
- 10) PHILIPPINE INSTITUTE OF VOLCANOLOGY AND SEISMOLOGY
- 11) Disaster Study Team of North Luzon Earthquake:
Report on the Disaster Caused by the 16 July 1990

Earthquake, 1990

- 12) Eiji Yanagisawa : Outline of Damage Caused by Philippine Earthquake, Papers in Symposium on Countermeasures against Liquefaction of Ground, P291, January 1991
- 13) Fudo's Total Foundation Engineering System :
Brochure of FUDO CONSTRUCTION CO., LTD.
- 14) Dynamic Consolidation Method : Brochure of Marine Engineering (Kaiyo Kogyo) Co., Ltd.
- 15) Japanese Society of Soil Mechanics and Foundation Engineering:
Countermeasure Method for Soft Ground, P125, 1990
- 16) Same as Ref. 15, P324
- 17) Co, Ltd. Industrial Survey Society (SANGYO CHOSAKAI):
Encyclopedia of Civil Engineering Methods, Fourth Edition, P 356, 1990

TABLES

Table 5.1 DAMAGED SHAPE OF RIVER DIKE

	Type I	Type II	Type III	Type IV	No Damage	Total
Number of Section	30	177	135	148	34	524
Percentage	5.7%	33.8%	25.8%	28.2%	6.5%	100%

Table 5.2 DAMAGED PLACES AND LENGTH IN EACH RIVER

River Name	River Dike		Revetment		Sluice Pipe	Weir	Total (Plac
	Place	Length (m)	Place	Length (m)			
Kitakami	13	7,902	4	444		1	18
Old Kitakami	2	224	4	74			6
Eai	4	610					4
Naruse	9	996			1		10
Yoshida	17	6,682			1		18
Natori	17	2,618	4	220			21
Abukuma	3	479	5	672			8
Total	65	19,511	17	1,410	2	1	85

Table 5.3 FEATURE OF DAMAGED DIKE

Feature River Name	Old River Channel	Closing Point of Old River	Crevasse	Soft Ground	Irregula Section
Kitakami	5	1		3	2
Old Kitakami					1
Eai	1				
Naruse	2	1		1	2
Yoshida	3	1	5	5	1
Natori	3		2	4	5
Abukuma		1		1	
Total	14	4	7	14	11

Table 5.4 DAMAGE QUANTITY OF RIVER DIKE

River Name	Number of Damage Place	Damaged Length (km)	Dike Length (km)	Damaged Rate (%)
Mabuchi	1	0.025	11	0.2
Iwaki	29	5.838	115	5.1
Yoneshiro	23	3.673	62	5.9
Omono	5	0.593	17 *	3.5
Mogami	4	0.296	56 *	0.5
Aka	1	0.016	59	0.03
Total	63	10.441	320	3.3

* length of downstream only

Table 5.5 DAMAGED DIKE BY CLASSIFICATION OF MICRO-TOPOGRAPHY

Micro-Topography Classifacation	Damaged Length (km)	Total Length (km)	Damage Rate (%)
Flood Plain	3.257	161	2.0
Micro-highland of Old River	2.376	56	4.2
Old River Channel	2.425	39	6.2
Natural Levee	0.197	30	0.7
Reclaimed Ground	1.321	10	13.2
Dune	0.016	8	0.2
Others	0.849	16	5.3
Total	10.441	320	3.3

Table 5.6 OCCURRENCE RATE OF SAND BOIL AT DAMAGED LOCATION OF RIVER DIKE

Micro-topographic Classification River Name	Natural Levee	Micro-highland of Old River	Dune	Old River Channel	Flood Plain	Reclaimed Ground	Others	Total	Occurrence Rate of Sand Boil
Iwaki	1/2	5/7	-	10/11	5/9	1/2	-	22/31	71
Yoneshiro	0/3	3/3	-	2/2	5/13	-	0/2	10/23	43
Downstream of Omono	-	-	-	1/1	0/3	-	-	1/4	25
Upstream of Omono	-	-	-	0/1	-	-	-	0/1	0
Downstream of Omono	-	-	-	0/1	0/1	-	-	0/2	0
Aka	-	-	0/1	-	-	-	-	0/1	0
Total	1/5	8/10	0/1	13/16	10/26	1/2	0/2	33/62	53
Occurance Rate of Sand Boil (%)	20	80	0	81	38	50	0	53	

Note: Upper value shows occurrence location number of sand boil.
 Lower value shows damaged location number of dike.
 The location which is classified into more than 2
 micro-topographic classification is counted for overlap.

Table 5.7 COMPARISON OF COMPACTION METHODS

Improvement Method	Suitable Ground	Required Material	Possible Depth of Improvement	Judgement
Sand Compaction Pile	Loose sand Silty particles are allowed a little	Sand Gravel Crusher-run	20 m- 30 m	○
Vibro Rod	Loose sand Sand contained silty particles more than 10 % is not effective	In place Sand	20 m	△
Vibro Tamper	Loose sand	No	3m	X
Vibro Flootation	Loose sand Sand contained much silt is not effective	Gravel Crusher-run	8m	X

Table 7.1 QUANTITY OF ADDITIONAL CORE BORING AND LABORATORY TEST

Area	Boring No.	Depth (m)	SPT	Sampling	Laboratory Test			
					GA	AL	NMC	SG
Dagupan City	DG 1	20.45	15	5	12	6	5	5
	DG 3	20.45	15	5	13	8	5	5
	DG 5	20.45	17	3	11	9	3	3
Middle Agno River	MA 2	20.00	7	2	10	5	3	3
	MA 5	20.45	15	5	10	4	4	4
	MA 6	20.45	16	4	10	6	4	4
Total		122.25	85	24	66	38	24	24

Note: SPT - Standard Penetration Test
 GA - Gradation Analysis
 AL - Atterberg Limits
 NMC - Natural Moisture Content
 SG - Specific Gravity

Table 7.2 PHYSICAL PROPERTIES OF GROUND IN DAGUPAN CITY AREA

Boring No.	Depth (m)	Fines Content (%)	D ₅₀ (mm)	Natural Moisture Content (%)	Plasticity Index	Specific Gravity	Unified Soil Classification
DG 1	1.15 - 1.45	88	-		32		GH
	2.0 - 3.0	15	0.17	28.0	NP	2.65	SM
	3.15 - 3.45	26	0.14				SM
	4.0 - 5.0	21	0.17	37.2	NP	2.64	SM
	5.15 - 5.45	21	0.16				SM
	7.0 - 8.0	22	0.20	24.4	NP	2.68	SM
	8.15 - 8.45	12	0.21				SM
	10.15 - 10.45	14	0.24				SM
	12.0 - 13.0	11	0.10	20.2	NP	2.69	SM/SP
	14.15 - 14.45	33	0.10				SM
16.0 - 17.0	24	0.12	19.6		2.77	SM	
19.15 - 19.45	84	-			8	CL	
DG 3	1.15 - 1.45	19	0.26		NP		SM
	2.0 - 3.0	16	0.22	26.6	NP	2.76	SM
	3.15 - 3.45	17	0.11				SM
	4.0 - 5.0	25	0.20	21.6	NP	2.59	SM
	5.15 - 5.45	21	0.16				SM
	6.0 - 7.0	23	0.16	23.7	NP	2.79	SM
	7.15 - 7.45	24	0.20				SM
	8.15 - 8.45	15	0.14				SM
	11.0 - 12.0	4	0.23	26.0	NP	2.60	SP
	13.15 - 13.45	6	0.20				SM/SP
16.0 - 17.0	21	0.20	25.3	NP	2.78	SM	
17.15 - 17.45	94	-			17	CL	
19.15 - 19.45	86	-			10	CL	
DG 5	1.15 - 1.45	15	1.5		NP		SM
	2.15 - 2.45	23	0.20		7		SC
	4.0 - 5.0	15	0.20	18.3	NP	2.64	SM
	5.15 - 5.45	15	0.21		NP		SM
	7.15 - 7.45	9	0.34				SM/SW
	9.0 - 10.0	18	0.18	11.2	NP	2.75	SM
	11.15 - 11.45	18	0.15				SM
	12.0 - 13.0	80	-	44.2	15	2.50	GH
	14.15 - 14.45	85	-			6	CL
16.15 - 16.45	70	-			18	CL	
19.15 - 19.45	87	-			11	CL	

Note: Fines Content: Silt and Clay content

D : Mean Particle Size (Particle size of percentage passing of 50%)

NP: Non Plastic

Table 7.3 PHYSICAL PROPERTIES OF GROUND IN MIDDLE AGNO RIVER BASIN

Boring No.	Depth (m)	Fines Content (%)	D (mm)	Natural Moisture Content (%)	Plasticity Index	Specific Gravity	Unified Soil Classification
MA 2	1.15 - 1.45	68	-				CL
	2.15 - 2.45	64	-		5		CL
	3.15 - 3.45	70	-				CL
	4.15 - 4.45	72	-				CL
	5.15 - 5.45	87	-		10		CL
	6.0 - 7.0	28	0.12	29.4	10	2.69	SC
	7.15 - 7.45	26	0.13				SC
	8.0 - 9.0	12	0.12	15.8	NP	2.59	SM
	9.15 - 9.45	13	0.19				SM
	12.0 - 13.0	2	6.3	18.6	NP	2.66	GW
MA 5	2.0 - 3.0	18	0.21	8.7	NP	2.77	SM
	3.15 - 3.45	21	0.23				SM
	4.15 - 4.45	19	-				SM
	5.15 - 5.45	13	0.20				SM
	6.0 - 7.0	16	0.26	20.9	NP	2.70	SM
	10.15 - 10.45	31	0.16				SM
	11.0 - 12.0	17	0.22	11.4	NP	2.68	SM
	13.15 - 13.45	22	0.21				SM
	15.15 - 15.45	9	0.18				SM/SW
	16.0 - 17.0	12	0.11	21.5	NP	2.71	SM
MA 6	1.15 - 1.45	15	0.19				SM
	2.0 - 3.0	24	0.11	33.6	NP	2.63	SM
	3.15 - 3.45	11	0.25				SM/SW
	4.15 - 4.45	8	0.21				SC/SW
	5.0 - 6.0	6	0.19	26.0	5	2.55	SC/SW
	6.15 - 6.45	91	-		29		CH
	7.15 - 7.45	97	-		26		CH
	10.15 - 10.45	18	0.18				SM
	11.0 - 12.0	17	0.21	17.0	NP	2.67	SM
	16.0 - 17.0	11	0.31	14.2	NP	2.63	SM/SW

Note: Fines Content: Silt and Clay content

D : Mean Particle Size (Particle size of percentage passing of 50 %)

NP: Non Plastic

Table 7.4 FEATURE OF SAND DEPOSIT

Area	Fines Content (%)	D (mm)	NMC (%)	Ip	Gs
Dagupan City	4 - 33 (17)	0.10 - 0.34	11-37	non plastic	2.59 - 2.79
Middle Agno River	6 - 31 (17)	0.11 - 0.31	11-34	non plastic	2.55 - 2.77

Note: Fines content: passing percentage under 0.074 mm, silt and clay
 () shows average value
 D : Mean particle size
 NMC: Natural Moisture Content
 Ip : Plasticity Index
 Gs : Specific Gravity

Table 7.5 COEFFICIENT OF UNIFORMITY AND CUPVATURE

Boring No.	Depth (m)	D ₆₀ mm	D ₁₀ mm	D60		(D30) ² Fines	
				UC = $\frac{D_{60}}{D_{10}}$	D30 mm	UC' = $\frac{(D_{30})^2}{D_{10} \times D_{60}}$	Content
DG3	11.0-12.0	0.26	0.12	2.2	0.18	1.0	4
DG3	13.15-13.45	0.23	0.09	2.6	0.13	0.8	6
DG5	7.15-7.45	0.38	0.10	3.8	0.24	1.5	9
MA2	12.0-13.0	0.8	0.12	6.7	1.7	3.0	2
MA5	15.15-15.45	0.20	0.085	2.4	0.15	1.3	9
MA6	4.15- 4.45	0.27	0.09	3.0	0.18	1.3	8
MA6	5.0 - 6.0	0.20	0.10	2.0	0.17	1.5	6

Remarks : * Sand and gravel

Uc : Coefficient of uniformity

Uc': Coefficient of curvature

Table 8.1 ASSUMED VALUE OF DENSITY AND MEAN PARTICLE SIZE
BY SOIL CLASSIFICATION

Soil Classification	Saturated Density Psat(t/m ³)	Wet Density Pt(t/m ³)	Mean Particle Size D (mm)
Surface Soil	1.7	1.5	0.02
Silt	1.75	1.55	0.025
Sandy Silt	1.8	1.6	0.04
Silty Sand	1.8	1.6	0.07
Very Fine Sand	1.85	1.65	0.1
Fine Sand	1.95	1.75	0.15
Medium Sand	2.0	1.8	0.35
Coarse Sand	2.0	1.8	0.6
Sand and Gravel	2.1	1.9	2.0

Table 8.2 LIQUEFIED DEPTH FROM GROUND SURFACE

Bore Hole No.	Depth from Ground Surface (m)
DG - 1	2.0 - 4.3 (2.3m), 7.3 - 12.1 (4.8m)
DG - 3	0 - 7.5 (7.5m)
DG - 5	0 - 5.6 (5.6m)
MA - 2	3.15- 7.7 (4.55m)
MA - 5	0 - 5.4 (5.4m), 10.9 - 12.4 (1.5m), 17.2 - 17.5 (0.3m)
MA - 6	0.3 - 6.0 (5.7m), 10.0 - 10.7 (0.7m), 15.0 - 18.4 (3.4m)

Note : () shows the thickness of liquefied layer

Table 9.1 COMPARISON OF COUNTERMEASURE METHOD AGAINST LIQUEFACTION

Principle	Method	Adoptable Depth	Effectiveness	Affection to Surroundings	Achievement	Unit Cost	Unit Cost Rate
Compaction	Sand Compaction Pile	GL - 35m	N value 25 - 30 FC less than 30%	Much vibration and noise	Many	Expensive	0.8
	Rod Compaction	GL - 20m	N Value 15-20 FC less than 15%-20%	Much vibration and noise	Many	Expensive	0.7
	Dynamic Consolidation	GL - 10m	Judged by Construction	Much vibration by tamping	Few	Expensive	0.7
Particle Size Improvement	Replacement	GL - 5m	Good result with gravel material	Stability and deformation of ground during excavation	Few	Moderate	
Mixing	Deep Mixing	GL - 30m	Due to mixing quantity of stabilizer material, improvement ratio	Less	Few	Very Expensive	5 - 6
Varying Stress	Counterweight Fill	-	Able to expect the effect	Land Acquisition	Many	Moderate	-
Dispersion of Excessive Pore Water Pressure	Gravel Drain Pile	GL - 20m	Unreliability of drain	Less	Many	Expensive	1.0
Confining of Deformation	Steel Sheet Pile	GL - 10m	Difficult to quantify	Vibration and noise by piling	Few	Very Expensive	3 - 4

Note : GL : Ground Level

FC : Fines Content

Table 9.2 COMPARISON OF COST OF COUNTERMEASURE METHOD

Countermeasure Method	Direct Cost per 1m of Earth Dike (Yen)	Unit Cost	Order
Sand Compaction Pile	128,900	3,410 /m	2
Dynamic Consolidation	196,800	7,570 /m ²	3
Deep Mixing	864,000	10,000 /m ³	5
Counterweight Fill	96,000	1,000 /m ³	1
Steel Sheet Pile	580,000	SPVL 27,000 /m ²	4

Note : 1) Cost of excavation and fill are not included.
 2) Cost of sand mat is not included.
 3) Cost of land acquisition is not included.

FIGURES

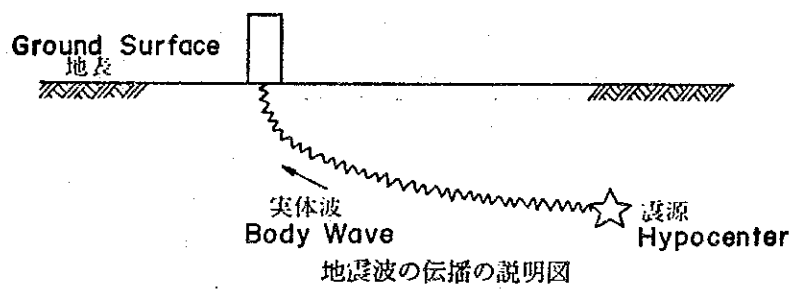


Fig. 3.1 EXPLANATION ON TRAVEL
OF EARTHQUAKE WAVE

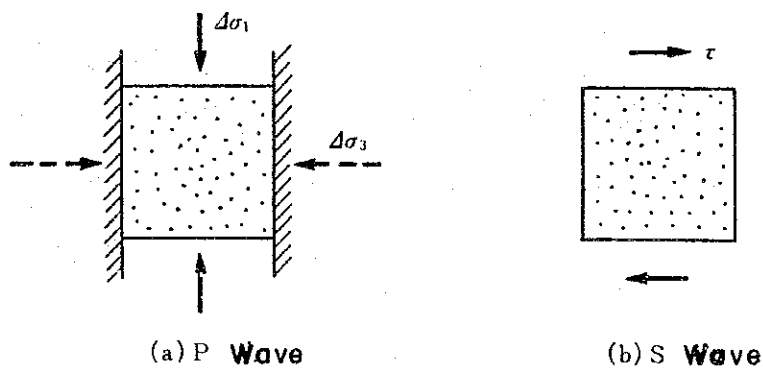


Fig.3.2 ACTING FORCE TO SOIL ELEMENT BY P WAVE AND S WAVE

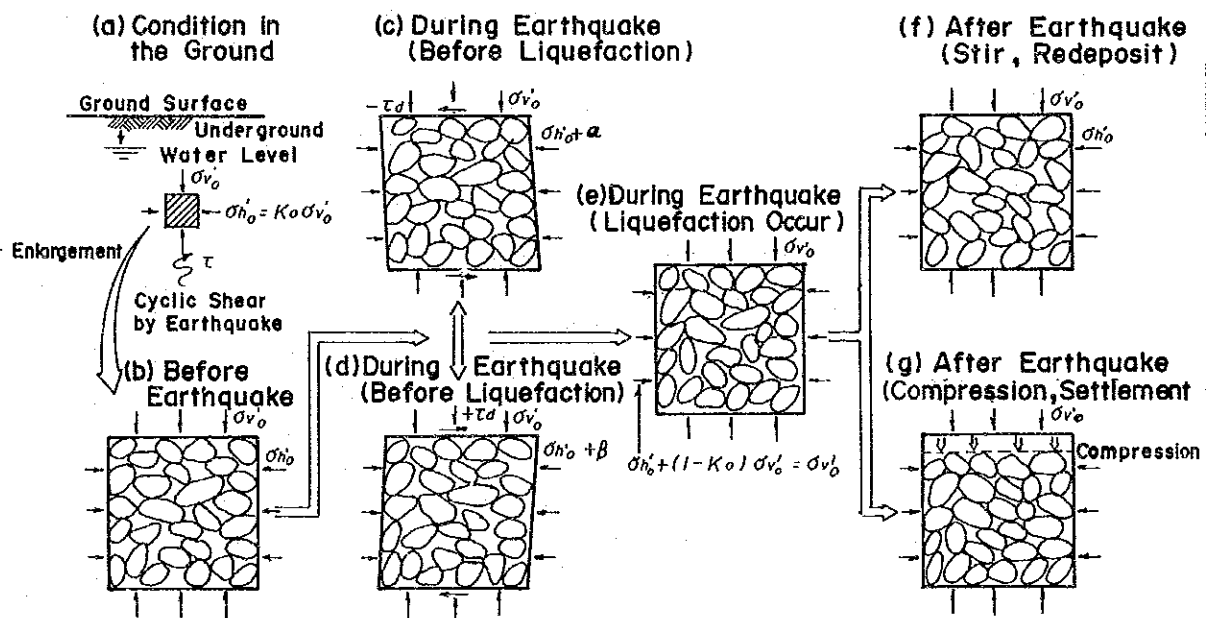


Fig. 3.3 LIQUEFACTION MECHANISM



(a) 地盤全体のすべり

Sliding of Ground

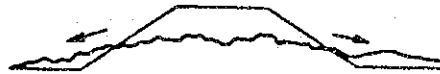
①すべり Slope Failure



②沈下 Settlement



③流出 Flow



(b) 土構造物

Earth Structure

Fig. 3.4 DAMAGE PATTERN INDUCED BY LIQUEFACTION